Temperature dependent removal of sodium chloride (NaCl) from synthetic nitrified urine

Samuel J. Huber

Master's thesis

Eawag: Swiss Federal Institute of Aquatic Science and Technology

Department of Process Engineering

Advisors:

Dr. Michael Wächter

Dr. Kai M. Udert

Prof. Dr. Eberhard Morgenroth

First submission: September 9, 2011

Submission of revised report: October 13, 2011

Submitted in partial fulfillment of the requirements for the degree of Master of Science in Civil Engineering (Diplomstudiengang Bauingenieurwesen) at the Karlsruhe Institute of Technology (KIT)

Summary

Urine is the source of the major part of plant nutrients in municipal wastewater. Therefore, full nutrient recovery from source-separated urine is an attractive option for both treating wastewater and gaining a valuable fertilizer product. Full nutrient recovery can be achieved by first stabilizing collected urine by nitrification and then concentrating the urine by distillation. Since concentrations of all salts in urine increase with increasing removal of water also the sodium chloride (NaCl) content is high in the end. There are two problems related to NaCl, the first being the synergistic decomposition of ammonium nitrate by chloride and the second being soil salinity and sodicity related problems when applying the product as fertilizer.

Solubility experiments using synthetic nitrified urine were carried out in the temperature range between 40 and 90°C. The synthetic urine solution contained seven inorganic ions at constant composition (NH_4^+, Na^+, K^+ // NO_3^-, SO_4^{2-}, PO_4^{3-}, Cl^- – H_2O). at different water contents in order to determine the achievable extend of NaCl removal. The aim was to find the conditions, at which a maximal amount of sodium chloride can be removed with minimal loss of other nutrients, especially nitrogen. The underlying hypothesis was, that the solubility of ammonium chloride (NH_4Cl) shows a much stronger temperature dependence compared to NaCl and therefore selective NaCl removal can be achieved at elevated temperatures.

The analysis of the solids showed, that mainly Cl^-, SO_4^{2-}, Na^- and to a lower extend NH_4^+ were present. At higher temperatures, more Cl^- relative to NH_4^+ was present in the solids. At 40°C, only NH_4Cl was found while for all temperatures above 60°C no NH_4^+ was observed at similar water contents. The maximal removal of sodium chloride was achieved at a water content of 7.1 % and was around 50 %. Na^+ removal was as high as 33 %. Nitrogen losses as NH_4Cl precipitate were around 11 %, while basically no potassium or phosphate was lost.

It was concluded, that selective removal of NaCl is possible at elevated temperatures. The maximal removal of Cl^-, however, might not be sufficient to affect ammonium nitrate decomposition significantly. With regard to soil salinization, the achieved NaCl removal might well have a relevant impact.

In order to rationalize results, two numerical models for electrolyte solutions, Pitzer and extended Uniquac, were applied. Both models could only give rough estimates for concentrations, at which crystallization started, as well as for the identities of solid phases. This result might be due to various reason, one being the very high ionic strengths in the nitrified urine system.

Some preliminary results for full nitrification using sodium hydroxide (NaOH) were obtained, and this process alternative circumventing the problem of ammonium nitrate decomposition is discussed.

Future investigations should focus on the following topics: the applicability of the results for synthetic urine on real urine; the effect of varying nitrogen contents in urine on NaCl removal; the mechanisms responsible for the loss of nitrogen during collection and storage of urine; full nitrification as an alternative process; further development of numerical models for electrolyte solutions at high ionic strengths.

Contents

List of Figures

List of Tables

Nomenclature

(aq)	Liquid state
(s)	Solid state
I	Ionic strength, $I = 0.5 \cdot \sum_{i=1}^{n} m_i z_i^2$
K	Solubility product (also denoted as K_{sp} in the literature)
SI	Solubility index
T	Temperature in °C
ΔG	Gibbs energy
$\Delta m_{tot}^{s}(T, c_w)$	Deviation of total mass of solids from the average for the condition T, c_w
Δz	Deviation of charge balance
$\bar{m}_{tot}^{s}(T, c_w)$	Average total mass of solids for the condition T, c_w
$\boldsymbol{\mu}$	Chemical potential
χ_i	Mole fraction of ion i, $\chi_i = b_i / \sum_{j=1}^{n} b_j$, $j = 1 \ldots n$
γ_i	Activity coefficient of ion i
$\mathcal{N}(\mu, \sigma^2)$	Normal distribution with parameters mean μ and variance σ^2
μ	Mean
σ^2	Variance
ε_i	Error of mass balance for ion i
a_i	Activity of ion i, $a_i = \gamma_i \cdot b_i$
b_i	Molality of ion i with units mol/kg H_2O
c	Axis intersection in linear curve $y = m \cdot x + c$
c_w	Water content in %
m	Slope in linear curve $y = m \cdot x + c$
m_i^{l}	Mass of ion i present in the liquid phase
$m_i^{residue}$	Mass of ion i present in wet residue as measured
$m_w^{residue}$	Mass of water in wet residue
$m_{tot}^{residue}$	Total mass of wet residue
$m_i^{solution}$	Mass of ion i present in solution as measured
$m_w^{solution}$	Mass of water in mother solution
m_i^{s}	Mass of ion i present in the solid phase
m_i^{tot}	Total mass of ion i initially added
n	Number of ions in the system

|	
sd	Standard deviation
z_i	Charge of ion i
CI_x	$x\,\%$ confidence interval
$\ln\mathcal{N}(\mu, \sigma^2)$	Log-normal distribution with parameters mean μ and variance σ^2
Var	Sample variance

1. Introduction

The majority of essential plant nutrients in municipal wastewater originate from urine. This corresponds to around 80 % of nitrogen (N), 50–80 % of phosphorous (P) and 80–90 % of potassium (K), respectively (Maurer et al., 2003; Kirchmann and Pettersson, 1995; Schouw et al., 2002). Separation of urine at the source not only allows for simpler and more effective wastewater treatment, it can also be used to create added value by harvesting nutrients contained in urine.

Methods for partial nutrient recovery from urine like struvite ($MgNH_4PO_4 \cdot 6H_2O$) precipitation are already employed (e.g. Etter et al., 2011), but they are very limited in the fraction of nutrients recovered. As struvite, 95 % or more of P can be recovered, but only 3 % of N (Pronk and Koné, 2009). As a means of maximizing the amount of the valuable product, full nutrient recovery from urine is being considered as a promising process (e.g. Maurer et al., 2006).

1.1. Process for full nutrient recovery from urine

The main process steps for full nutrient recovery from urine is depicted in **Fig. 1**. Urine can be separated at the source, e.g. using waterless urinals and NoMix toilets and collected in storage tanks. Stored urine is characterized by a pH value of about 9, which results from the biological decomposition of the main nitrogen compound urea ($NH_2(CO)NH_2$) to ammonia (NH_3), ammonium (NH_4^+) and bicarbonate (HCO_3^-) (Udert et al., 2003b). At this pH, the ammonium-ammonia equilibrium is strongly shifted to the ammonia side, which favors loss of nitrogen through volatilization. Most of the Calcium (Ca^{2+}) and Magnesium (Mg^{2+}) precipitate as phosphates and carbonates. In order to avoid nitrogen loss, stored urine can be stabilized by nitrification, the biological oxidation of ammonium to nitrate (Udert et al., 2003a, 2005). During this process, the pH decreases from 9 to values between 6 and 7. Additionally, 90% of organic substances are degraded by heterotrophic bacteria.

The overall equation of the two step process of nitrification can be formulated as follows:

$$NH_4^+ + 2\,O_2 \longrightarrow NO_3^- + 2\,H^+ + H_2O \tag{1}$$
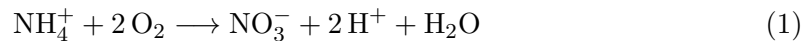
The pH decreases during nitrification due to alkalinity consumption (two H^+ are formed
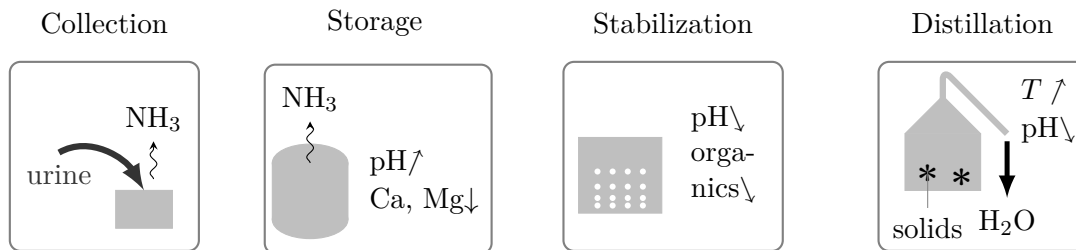

Fig. 1: Process steps of the treatment of separated urine for full nutrient recovery. $\nearrow$ and $\searrow$ indicates an increase and decrease, respectively, $\downarrow$ indicates precipiation.

1

per mole NH_4^+ oxidized), as can be seen from equation (1). Without addition of chemicals to balance consumed alkalinity, nitrification is inhibited and only about 50% of NH_4^+ is oxidized to NO_3 (Udert et al., 2006).

After nitrification, the stabilized urine is concentrated by distillation at temperatures above 60°C. If nearly all water is removed, a solid product can be obtained. Because of the high temperature, the decrease in pH and the high salt concentration, the urine is assumed to be sanitized (Udert and Wächter, 2011).

In this work, nitrified urine is mimicked by a synthetic electrolyte solution containing seven ions (Na^+, K^+, NH_4^+, NO_3^-, Cl^-, SO_4^{2-} und PO_4^{3-} in H_2O). The composition, which was adopted from Udert et al. (2006), can be found in **Tab. 1** on page 8.

1.2. Problems related to sodium chloride

There are two known problems related to NaCl, the first one being autocatalytic decomposition of ammonium nitrate with chloride and the second one soil salinization when applying the product as fertilizer.

1.2.1. Decomposition of ammonium nitrate

It has long been known that NH_4NO_3 decomposes at elevated temperatures (Saunders, 1922). The main reaction of this decomposition is the following:

$$NH_4NO_3 \longrightarrow N_2O + 2H_2O \qquad (2)$$

The peak temperature of pure NH_4NO_3 determined by differential scanning colorimetry (DSC) is about 326°C according to Oxley (2002). Already Saunders (1922) found the accelerating effect of Cl^- on the NH_4NO_3 decomposition, at concentrations as low as 0.1 %. In addition to the accelerating effect Oxley (2002) quantified a decrease of the peak temperature by Cl^- of about 70°C.

Many more studies have shown the destabilizing effect of Cl^-, which acts as an autocatalyst. The key step in the destabilization is suggested (e.g. by Keenan et al., 1969) as

$$NO_2^+ + Cl^- \longrightarrow NO_2 + Cl \qquad (3)$$
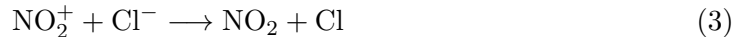
However, there is no consensus in the literature on the reaction mechanism.

An additional accelerating effect has been reported for acids, e.g. HNO_3, on the induction period of the catalytic activity of Cl^- (Wood and Wise, 1955; Rubtsov et al., 1989).

Keenan et al. (1969) found in a survey of two dozen metals, that this synergistic catalysis might require, besides Cl^-, the presence of a metal, which has the following properties: It needs to be able to exist in at least two oxidation states, which are separated by a one-electron jump and needs to allow for the formation of moderately stable chloro complexes. This is for example true for copper. Chromium was found to have the strongest catalyzing effect. The catalyzing effects were found at metal concentrations of less than 0.1 % and mole ratios of Cl^- and NH_4NO_3 of 0.05.

Equivalently to the effect of acids, bases such as phosphates or carbonates generally retard the decomposition of ammonium nitrate. Calcium carbonate shows the largest effect. It was reported that the peak temperature increased by about $60°C$ with addition of 20% $CaCO_3$. In addition to acid, urea was found to have a stabilizing effect on ammonium nitrate (Oxley, 2002).

Small amounts of water of around 5% generally inhibit the decomposition. However, MacNeil et al. (1997) described how besides solid NH_4NO_3 compounds, aqueous NH_4NO_3 in hot solutions bear a potential for decomposition.

There has been a remarkable number of severe accidents with NH_4NO_3 products involved (Oxley, 2002). In order to account for the dangers of the autocatalytic reaction of ammonium nitrate, the EU set strict regulations for fertilizers (European Parliament and European Council, 2003). N-content (as ammonium nitrate N) larger than 28%, Cl content lower than 0.02%, total organic carbon (TOC) below 0.4% and pH of at least 4.5 in a solution of 10 g of product in 100 ml.

1.2.2. Soil salinization

Soil salinity is the amount of salt contained in a soil. It is also referred to as a soil condition, which is characterized by an excess of salts. Natural sources of salts in soils include weathering of parental rocks, accumulation of salts in arid and semiarid zones and deposition of oceanic salts by wind and rain (Munns and Tester, 2008). A very common source is irrigation water, which usually contains salts (Brouwer et al., 1985).

Salt levels of soils are assessed using the electric conductivity of the saturated paste extract (EC_e) and the sodium adsorption ratio (SAR). The SAR is defined as SAR = $C_{Na^+}/(C_{Ca^{2+}} + C_{Mg^{2+}})^{0.5}$ and reflects the relative abundance of sodium at the cation exchange sites of the soil (Soil Science Society of America, 1997). Numerical criteria for these two widely used categories are $EC_e \geq 4\,mS/cm$ for saline soils and SAR > 13 for sodic salts (Soil Science Society of America, 1997; Richards, 1954). If the salinity and sodicity criteria are both exceeded, the soil is called saline-sodic.

Adverse effects of salts in soils include reduction in plant growth rate, reduced crop yield and even total crop failure (Qadir et al., 2000). An important reason for these effects is the increasing osmotic pressure with increasing salt concentrations, which reduces the uptake rate of water in the plant. Other reasons are related to specific ions. Chloride and Sodium may be directly toxic to plants with various related effects (Bernstein, 1975). A high sodicity negatively affects the soil's physical and chemical properties and leads to poor soil structure, low infiltration rate, poor aeration and makes the soil difficult to cultivate (Qadir and Schubert, 2002). Additionally, sodicity can lead to nutritional deficiencies for Ca and Mg (Bernstein, 1975). In an extensive review on the relations between salinity and mineral nutrition of crops, Grattan (1998) points out that nutrient additions above the non-saline considered levels might be beneficial, e.g. correcting Na-induced Ca^{2+} deficiencies by supplemental calcium.

Tolerance of crops to excess salts in soils varies widely. While some halophilic plants are capable of tolerating root zone salinity levels from several hundreds up to $1000\,mM$, the growth of non-halophilic plants is severely inhibited already around $50\,mM$. Basically

all major crops are non-halophilic (Volkmar et al., 1998).

There is a number of studies in the literature investigating the use of urine as fertilizer. Mainly untreated, stored urine was used. Many of these studies relate lower yields observed for urine fertilized plants compared to those treated with commercial NPK fertilizer to the high sodium chloride content in urine (Ganrot et al., 2007; Mnkeni et al., 2008, 2005; Simons and Clemens, 2003). None of these studies, however, shows clear evidence for this correlation.

Very recently, two studies on application of untreated human urine as fertilizer pointed out the potential implication of high chloride concentrations to the yield. Germer et al. (2011) pointed out, that further investigations on the long-term effects of NaCl contained in urine on crops are needed and Pradhan et al. (2009) concluded additionally, that the low K content in urine might explain lower yields compared to commercial NPK fertilizer.

1.2.3. Removal of sodium chloride

Various processes for separating components of electrolyte solutions exist. Some examples for such processes employed in practice are evaporative crystallization, hot dissolution, fractional crystallization, ion exchange columns and membrane processes.

Simple systems like a solution containing NaCl and KCl can be separated relatively easy. If the goal is to only remove some sodium chloride, evaporative crystallization can be employed. In this process, water is removed from the solution, e.g. by distillation, and the solution is then cooled to a temperature, at which KCl solubility is larger than that for NaCl. This process is frequently employed to get NaCl from sea water, by simply feeding it to salt evaporation ponds, where natural evaporation leads to crystallization of salts. By controlling the separation pathway, the extend of NaCl separation can be increased (e.g. Cohen-Adad et al., 2002).

The hot dissolution process is frequently employed to separate e.g. KCl from other rocksalts. This is done by dissolving the raw salts in a solution saturated with the rocksalts at high temperatures. KCl dissolves and the residue salts can be removed by filtration. Upon cooling very pure KCl is attained from the solution.

Ion exchange is widely used, usually in form of ion exchange columns containing synthetic resins specific to the application purpose. This process is employed e.g. in waste water treatment but also for chemical analysis or protein purification.

Very recent advances in separation of electrolyte solutions come from membrane technologies. Mir and Shukla (2010) for instance employed the effect of negative rejection of NaCl observed using an ultra filtration membrane for separating a solution containing NaCl and KCl.

Despite the large variety of separation processes, a crystallization process is investigated in this work because of its relative simplicity and robustness. These are desired properties for a nutrient recovery process from urine, which has its largest application potential in developing regions of the world.

1.3. Theoretical background

An electrolyte solution contains two or more ions, the solutes, and water, the solvent. The liquid phase can be in thermodynamic equilibrium with none, one or several solid phases, depending on composition, temperature and number of components in the system. As an example of an equilibrium reaction, the solid liquid reaction for solid NaCl and its dissociated aqueous species Na^+ and Cl^- can be written as follows:

$$NaCl(s) \rightleftharpoons Na^+(aq) + Cl^-(aq) \tag{4}$$
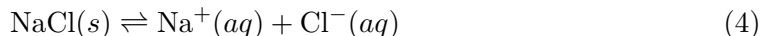
The criterion for the thermodynamic equilibrium of any component in an electrolyte solution is the equality of the chemical potentials in the phases it is present, i.e.

$$\boldsymbol{\mu}_{NaCl} = \boldsymbol{\mu}_{Na^+} + \boldsymbol{\mu}_{Cl^-} \tag{5}$$

This condition satisfies the minimal Gibbs Free Energy in the system.

Electrolyte solutions, if they are not very dilute, are highly unideal solutions due to the interactions of the ions. Therefore, molalities b_i and activities $a_i = b_i \gamma_i$ in units mol/kg H_2O are used. γ_i is the activity coefficient, which represents the deviation from ideality.

The solubility product for the the solid liquid equilibrium K_{NaCl} can be computed from the standard chemical potentials of the solid salts and its liquid constituents. The degree of saturation of the solution with respect to a salt such as NaCl is given by the solubility index, which is the ratio between the activity product of the salt and the its solubility product:

$$SI_{NaCl} = \frac{a_{Na^+} \cdot a_{Cl^-}}{K_{NaCl}} \tag{6}$$

Whether the thermodynamic equilibrium of a system is reached and after what time depends on the kinetics of the equilibrium reactions. The driving force for crystallization is oversaturation of the solution with respect to one component. Since the initial formation of a crystal nucleus requires some activation energy, metastable equilibria are possible, i.e. with one component in oversaturation, which may prevent the system from reaching the thermodynamic equilibrium.

The ionic strength $I = 0.5 \cdot \sum_{i=1}^{n} b_i z_i^2$ as a measure of the concentration of ions is an important concept, which is widely used in models. In the Debye-Hückel theory I plays a central role (Debye and Hückel, 1923, cited in Thomsen (1997)). The Debye-Hückel law can accurately describe dilute electrolyte solutions up to $I = 0.01$ mol/kg H_2O. For solutions of concentrations up to $I = 0.5$ mol/kg H_2O, the Davis equation represents an empirical extension of the Debye-Hückel law. For higher ionic strengths, the Pitzer model (Pitzer, 1973) and extended UNIQUAC (Thomsen et al., 1996; Thomsen, 1997) are two currently employed models with potential for the simulation of high ionic strength solutions. Both use a significant number of parameters.

1.4. Aim of the work

Solubility experiments with synthetic nitrified urine containing seven inorganic ions at constant composition (NH_4^+, Na^+, K^+ // NO_3^-, SO_4^{2-}, PO_4^{3-}, Cl^- – H_2O) at different water contents and temperatures were conducted. The aim of the work was to find out whether it is feasible to remove chloride as sodium chloride using crystallization at high temperature.

This work was based on the following hypotheses:

- Sodium chloride can be removed selectively at elevated temperatures due to the small temperature dependence of its solubility compared to ammonium chloride. The temperature dependences of the solubility of NaCl and NH_4Cl are depicted in **Fig. 2**.

- It is not possible to remove chloride completely, since with increasing removal of chloride, increased precipitation of other species like ammonium or sulfate is expected.
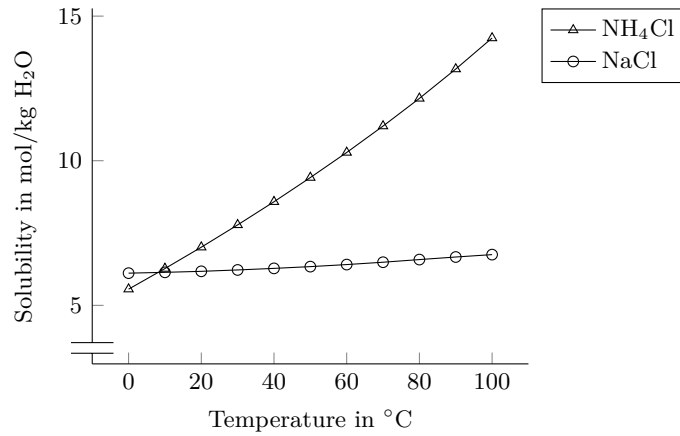
Fig. 2: Solubilities as molalities for NH_4Cl and NaCl between 0 and 100°C. Values were taken from Lide.

2. Methods

2.1. Experimental method

The solubility experiments were conducted using a direct method with analysis of both mother solution and residue. Salts and stock solution were synthesized with constant salt composition and varying water contents according to **Tab. 1**. An overview of equilibration and sampling is given in **Fig. 3**. In the following, a rather short description of

(a) vessel with lid and septum

(b) addition of salts

(c) addition of water

(d) equilibration at $T°$

(e) sampling of mother solution

(f) immediate dilution of solution

(g) wet residue

(h) drying of residue
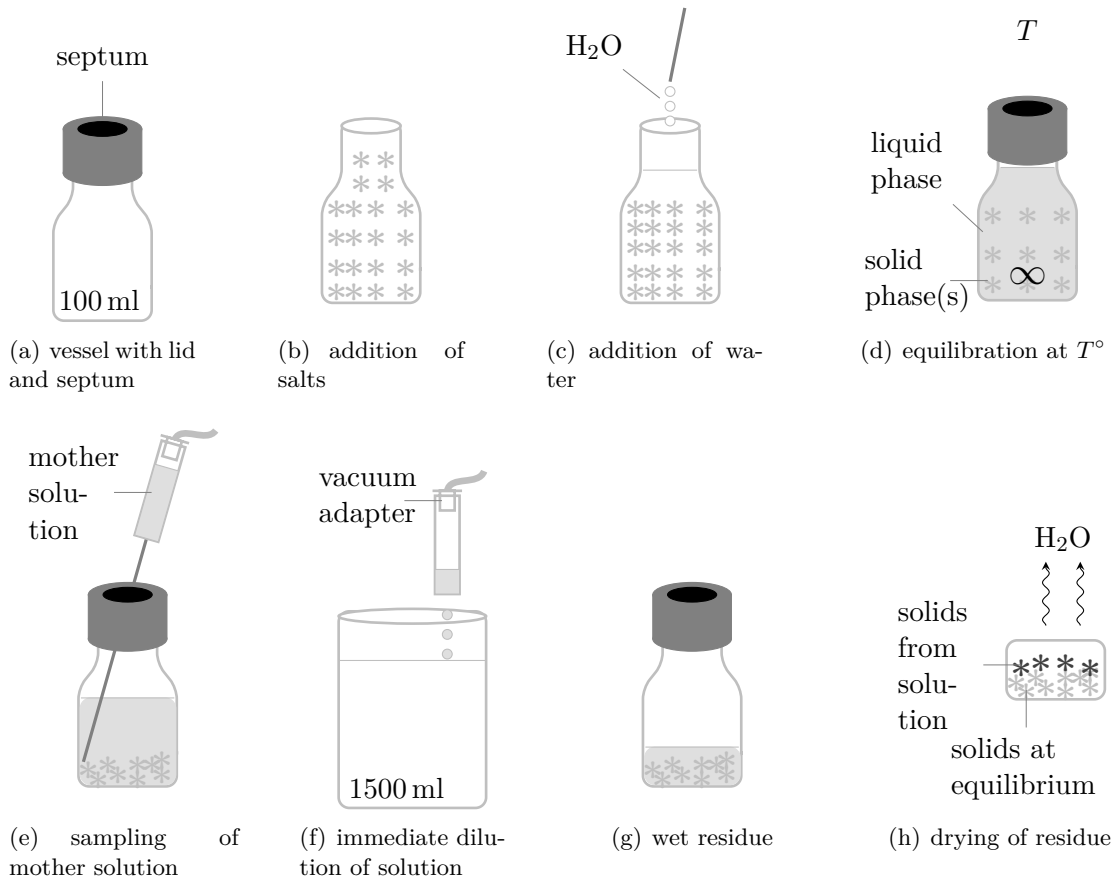
Fig. 3: Overview of experimental method. Vessels of 100 ml volume with septa (a) were filled with salts (b) and water (c) according to salt composition and water content c_w of interest. The vessels were closed and equilibrated at temperature T in an oil bath. Mixing was achieved by magnetic stir bars (d). After typically 70 h, mixing was stopped to allow for settling of the solids. The liquid phase was then sampled as the mother solution using a 50 ml syringe and a long needle while the vessel remained at T (e). The mother solution was weighed and immediately diluted in 1000 to 1500 g of water in order to keep all ions dissolved in the mother solution in solution (f). The wet residue, which remained as a mixture of solids and remaining mother solution in the vessel (g), was dried by lyophylization until constant weight was reached (h).

Tab. 1: Composition of synthetic nitrified urine. The investigation of the partially nitrified system from nitrification with no addition of chemicals was the main objective of the work. In order to discuss process alternatives, two hypothetical composition of fully nitrified urine are given additionally, in which NaOH and CaCO$_3$, respectively, are added during nitrification in order to balance alkalinity consumption.

Species	Unit	Partial nitrification	Full nitrification NaOH	Full nitrification CaCO$_3$
NH$_3$-N	mg/l	3360	0	0
NO$_3$-N	mg/l	3360	6700	6700
PO$_4$-P	mg/l	530	530	530
SO$_4^{2-}$	mg/l	1540	1540	1540
CO tot	mg/l	650	650	15300
Cl$^-$	mg/l	3900	3900	3900
Na$^+$	mg/l	2530	13600	2530
K$^+$	mg/l	2200	2200	2200
Ca^{++}	mg/l	0	0	9600
pH (set)	-	6.0	6.0	6.0
Alkalinity *	mmol/l	6	8	125
c_w	%	96.9	94.9	93.5

* simulated values using EQ3/6

the method is given. A more detailed description can be found in appendix A.6 on page 36 ff..

For each condition (defined by water content c_w and temperature T), 3 to 4 duplicates were run in parallel. The total mass of solution prepared for equilibration was between 140 and 160 g. All chemicals added were of grades "purissimum" or "pro analysis". For equilibration, two oil baths consisting of a crystallization beaker with polypropyleng-lycole and a magnetic stirrer with contact thermometer were used. The temperature accuracy of the system was about $\pm 1°$C. For sampling, a needle (200 mm $\times$ 2 mm) connected to a 50 ml syringe was pushed through the septum and then lowered along the vessel wall with the open side of the needle tip facing the wall in order to minimize removal of solids (compare **Fig. 3(e)**).

Extraction of the mother solution was achieved by attaching a vacuum pump via an adapter to the syringe. The mass of the mother solution, m^{solution}, was determined and it was immediately diluted in 1 to 1.5 kg of water. After removal of most of the mother solution, the vessel with the remaining wet residue was taken out of the oil bath, rinsed on the outside with hot water and mixed manually using a spatula. At room temperature, the residue was typically solid. After determining the residue's mass, m_{tot}^{residue}, 7 to 20 g of the residue were transferred into a tube for drying by lyophilization. Freezing of the residue samples was achieved by either shock freezing using liquid nitrogen for around one minute or keeping them in the freezer at -80°C for at least two hours prior to putting them to the lyophilization apparatus.

For chemical analysis of cations and anions, ion chromatography (IC) was employed. Prior to analysis, the initially diluted mother solution samples were additionally diluted

5 to 7 times and the dried residue samples were pestled and about $1\,g$ was diluted in $100\,ml$ of ultra pure water.

2.2. Evaluation of experimental results

The evaluation of the experimental results was done in terms of mass balances for each ion i in the system. A schematic representation of the different quantities involved in these mass balance calculations can be found in **Fig. 4**.

An over all mass balance for ion i can be formulated as follows:

$$m_i^{tot} = m_i^l + m_i^s \quad \text{for all} \quad i = 1 \dots n \tag{7}$$

where m_i^{tot} is the total mass in the system, m_i^l the mass in the liquid phase and m_i^s the mass in the solid phase. m_i^{tot} is given by the initial addition of each ion.

For the experimental sampling, the following balance applies:

$$m_i^{tot} = m_i^{solution} + m_i^{residue} + \varepsilon_i \tag{8}$$

with mass of ion i as determined by chemical analysis in the mother solution, $m_i^{solution}$, and in the residue, $m_i^{residue}$.

Two methods are employed in order to calculate the amounts as liquid and solid for each ion.
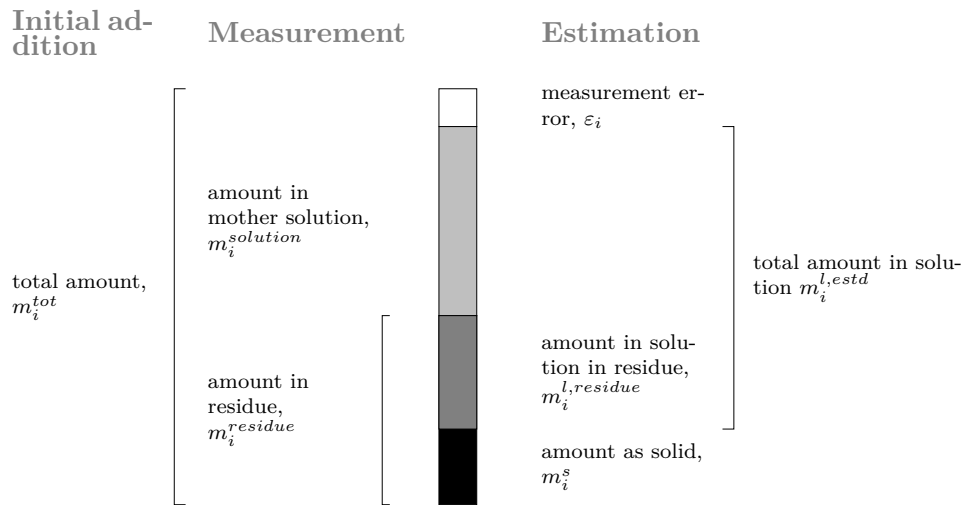
Fig. 4: Schematic representation of the mass balance applied to each ion i ; The different proportions of the mass balance are given as masses in gram. From left to right, three dimensions of the mass balance analysis are depicted: the total mass present, which equals the amount initially added; the measured quantities of solution and residue, determined by chemical analysis; the estimated quantities of liquid and solid, which were determined using the measured quantities. The error was determined as deviation of the mass measured from the mass initally added.

Water content Using the water contents of residue and mother solution, $m_w^{residue}$ and $m_w^{solution}$, the amount of ion i in solution in the residue, $m_i^{l,residue}$, can be computed as follows:

$$m_i^{l,resdiue} = \frac{m_w^{residue}}{m_w^{solution}} \cdot m_i^{solution} \tag{9}$$

The amount of water in the solution is obtained as the difference between the total mass of the solution, $m^{solution}$, and the mass of the ions in the solution:

$$m_w^{solution} = m^{solution} - \sum_{j=1}^{n} m_j^{solution} \tag{10}$$

Using the identities $m_i^{residue} = m_i^{l,residue} + m_i^s$, the amount of each ion as solid can be estimated as follows:

$$m_i^s = m_i^{residue} - \frac{m_w^{residue}}{m_w^{solution}} \cdot m_i^{solution} \tag{11}$$

$$= m_i^{residue} - \frac{m_w^{residue}}{m^{solution} - \sum_{j=1}^{n} m_j^{solution}} \cdot m_i^{solution} \quad \text{for all} \quad i,j = 1\ldots n \tag{12}$$

And the amount in solution follows as:

$$m_i^l = m_i^{solution} + m_i^{l,residue} \tag{13}$$

NO_3 as reference species Under the assumption, that NO_3^- does not precipitate under the conditions examined, NO_3^- can be used as reference ion and the amounts of each ion in the residue composition coming from the liquid phase can be determined as follows:

$$m_i^s = m_i^{residue} - \frac{m_{NO_3}^{residue}}{m_{NO_3}^{solution}} \cdot m_i^{solution} \quad \text{for} \quad i = 1\ldots n \tag{14}$$

The total amount in solution, m_i^l, is determined using equation (13).

2.3. Error analysis

Based on mass balances, errors for each ion ε_i as deviations of the measured and initally added masses can be obtained according to equation (8):

$$\varepsilon_i = m_i^{solution} + m_i^{residue} - m_i^{tot} \tag{15}$$

Since the error of the weighed initial masses of ion i, $m_i^{ini} = m_i^{tot}$, were with $\pm 0.05\,\%$ approximately 2 orders of magnitude smaller compared to measured quantities of the samples, they were taken as quantities free of error.

In addition to the analysis of mass balances for each ion, the charge balance for the estimated solids were computed as an additional means of evaluating the quality of

the experimental data. The charge balance deviations were computed for each single experiment as:

$$\Delta z = \frac{\sum_{i=1}^{n} b_i \, z_i}{\sum_{i=1}^{n} b_i} \tag{16}$$

All experiments were evaluated using both methods for estimating the amounts of each ion in the liquid and the solid phase as described in section 2.2. Each method was evaluated by Monte-Carlo analysis (MCA) for determining the error propagation in the calculations of ions in solid and liquid phases.

In the MCA, for each quantity in the computation of solids and liquids as described in section 2.2, normal distributions of the errors ε_i as $\mathcal{N}(\mu_i = \bar{\varepsilon}_i, \sigma_i^2 = \mathrm{Var}(\varepsilon_i))$ were used for each ion. The mean μ_i represents the bias of the measurements for ion i, the variance σ_i^2 represents their variation.

Due to the nature of the experimental method, differing solid masses m_{tot}^s of the replicates at the same conditions were observed. The relative deviations of the total mass as solid of each replicated experiment at some T and c_w, $\Delta m_{tot}^s(T, c_w)$, were computed using the difference between the mass of solids of each replicate, $m_{tot}^s(T, c_w)$, and the average of the solid masses of all replicates, $\bar{m}_{tot}^s(T, c_w)$:

$$\Delta m_{tot}^s(T, c_w) = \frac{m_{tot}^s(T, c_w) - \bar{m}_{tot}^s(T, c_w)}{m_{tot}^s(T, c_w)} \tag{17}$$

In order to account for these variations in the MCA, the computed quantities m_i^s and m_i^l were multiplied by a factor α. A log-normal distribution of α as $\ln\mathcal{N}(\mu_i = 1, \sigma_i^2 = \mathrm{Var}(\Delta m_{tot}^s))$ was used.

In the computations of the MCA, absolute mass values were used. The computation of the mass of each ion in solid and liquid state was done by applying the distributions of the error of the mass balances, ε_i, and of the deviations of the total solid masses, Δm_{tot}^s, as percentages. 5000 random samples for all quantities were drawn from the given distributions. As the result of the analysis, the distributions of the means of the estimated values of m_i^l and m_i^s for each experimental condition were obtained. As robust estimators for representing these distributions, the median and the 10 % and 90 % quantiles were computed to obtain the 80 % confidence intervals.

For more details about the error analysis, refer to the digital resources, described in appendix A.1. The statistical analysis was done using R: A Language and Environment for Statistical Computing (R Development Core Team, 2003).

3. Results

First, the results obtained for the main system investigated, synthetic nitrified urine, are presented. The focus is set on the solids, but also results for the solution are shown. Next, results with regard to reaching the thermodynamic equilibrium are given. Additionally, results for the preliminary investigation for full nitrification are presented. The final part of this section is devoted to the statistical analysis of the results.

3.1. Solids

The percentages for each ion found as solid at all experimental conditions evaluated are depicted in **Fig. 5**. These percentages are equivalent to the possible removal for each species. At all temperatures between 60 and 90°C, basically no NO_3^- and PO_4^{3-} and only very low amounts of K^+ were found in the solids. Only for a water content of 9 % at 60°C, PO_4^{3-} and K^+ were present as solids, which might be due to insufficient mixing and equilibration achievable at this combination of high concentration and low temperature. The highest percentages were observed for Cl^-, SO_4^{2-}, Na^- and to a lower extend NH_4^+.

Generally, for equal water contents, decreasing amounts of the ions with increasing temperature would be expected due to increasing solubilities for most of the components. However, when a phase change occurs, a different trend might be seen. When comparing the percentages of NH_4^+ at equal water contents but different temperatures, it can be seen that the amount of NH_4^+ decreases as temperature increases. For Na^+ in contrast, there is rather an opposite trend.

In order to compare the solid NaCl and NH_4Cl, the mole numbers of NH_4^+ in the solids were compared to those of Cl^-. The resulting plots are displayed in **Fig. 6**. The diagonal dashed line in each subgraph represents equimolar amounts of NH_4^+ and Cl^-. A significant trend can be seen for increasing temperature in that the slope of the linear regression of different water contents at a temperature decreases from values of 0.9 to 0.58 mol NH_4^+/mol Cl^-. Additionally, except for 40°C, there was no NH_4^+ found in the solids at the lowest concentration. These observations suggest, that at low concentrations, Cl^- can be selectively removed as NaCl, while only at higher concentrations additionally NH_4Cl is present. The relative proportion of NH_4Cl to NaCl also decreased with increasing temperatures, the linear regression lines move horizontally in positive x axis direction. At 40°C, in contrast, NH_4Cl and no NaCl is present (triangular mark in **Fig. 6(d)**).

The components in the solid phases were not determined by direct measurements, but they could only be deduced from the relative compositions of the solids. In **Fig. 7**, the mole fractions of the solids for different water contents at different temperatures are depicted. As already described, only Cl^-, SO_4^{2-}, Na^-, NH_4^+ and in a few cases K^+ were observed in the solids in quantities sufficiently high for graphical display. In the upper left area of the graph, the phase change from NH_4Cl at 40°C to NaCl at 60°C is clearly visible. For the same temperature and increasing concentrations, first an increasing and then relatively constant mole fraction of NH_4^+ can be seen.
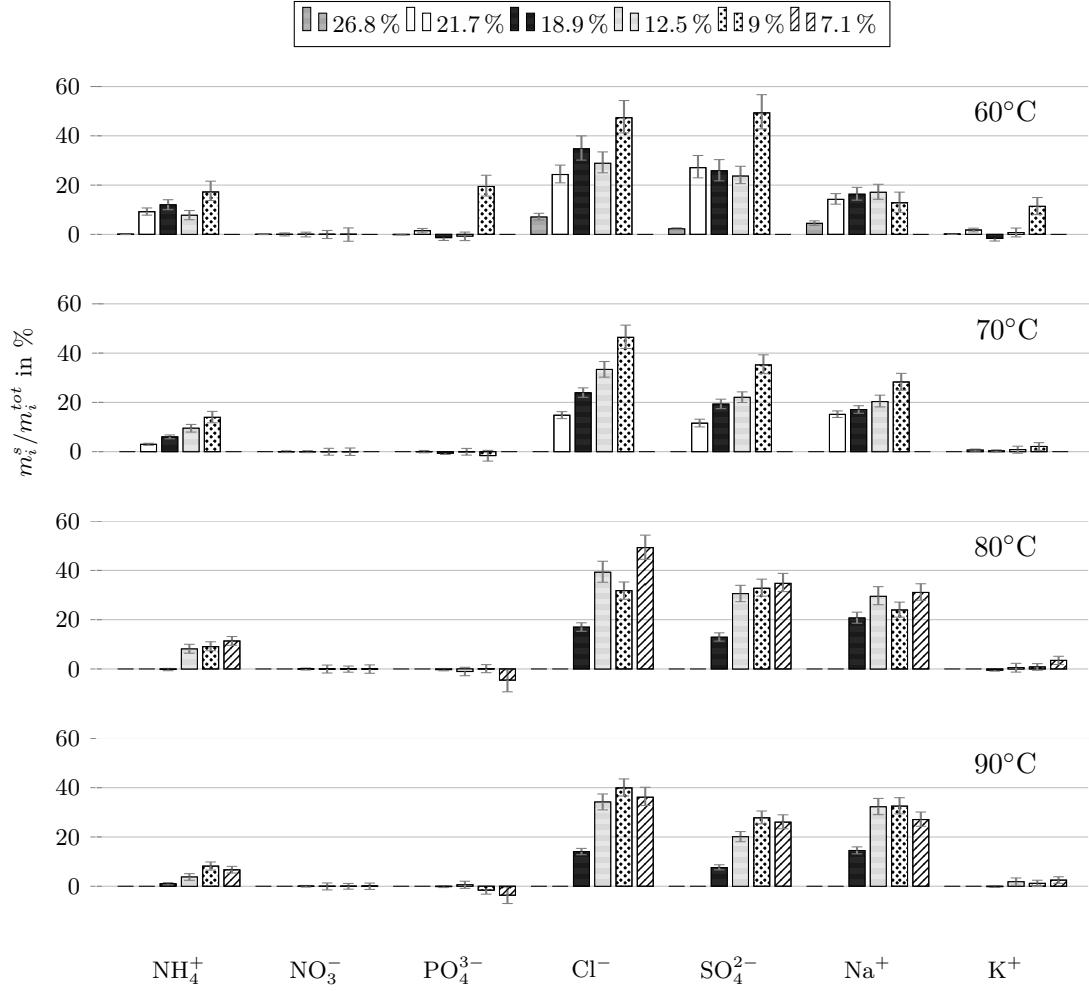
Fig. 5: Barplots of percentage for each ion as solid at different experimental conditions; Total water contents c_w were between 26.8 and 7.1 %, indicated by different patterns of the bars, and temperatures ranged between 60 and 90°C. The same water contents at different temperatures are aligned vertically. If no experiment at a specific water content was conducted at a temperature, the bars were simply set to zero. The error bars depict the 10 and 90 % quantiles obtained from MCA.
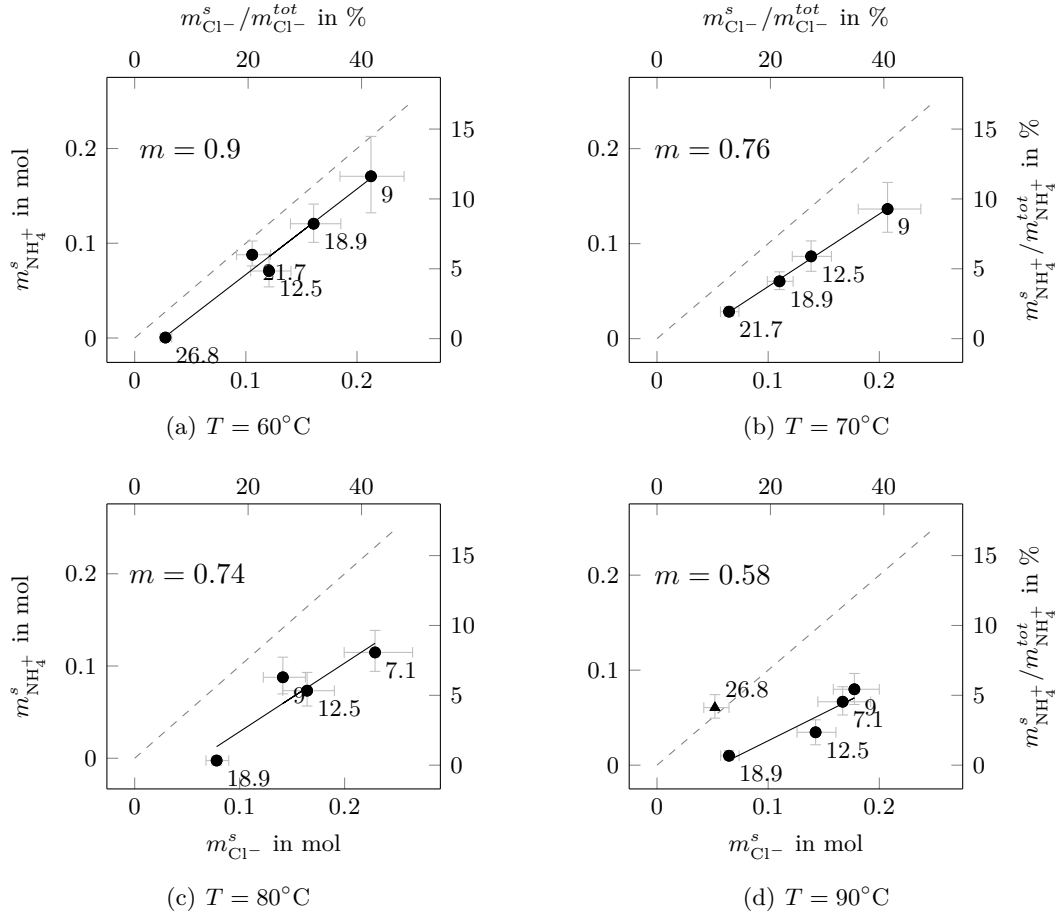
Fig. 6: Scatter plots of mole numbers of solid NH_4^+ against solid Cl^- for temperatures from 60 to 90°C. Left and lower axes represent the amount of solid NH_4^+ and Cl^-, $m_{NH_4^+}^s$ and $m_{Cl^-}^s$, in mole numbers, and right and upper axes the according percentages of the total amount of each ion. Figures at the coordinates denote the total water content c_w in %. The error bars depict the 10 and 90 % quantiles obtained from MCA. The triangular mark in (d) represents an experiment at 40°C, in which NH_4Cl was observed as the only solid phase.

14

χ_i

Legend: NH_4^+ K^+ Na^+ SO_4^{2-} Cl^-

40°C: 3.2, 0, 0, 0, 0, 0

60°C: 1.6, 8.7, 11.1, 8.7, 17.4, 0

70°C: 0, 5.1, 8.1, 9.9, 15.1, 0

80°C: 0, 0, 5.7, 11.8, 11.3, 15.8

90°C: 0, 0, 4.5, 10.2, 12.9, 11.8

c_w in %: 26.8, 21.7, 18.9, 12.5, 9, 7.1

Fig. 7: Composition of solid phases as mole fractions for different water contents and temperatures. Numbers above the bars depict the average total mass of solids in gram. If the absolute mole numbers of one species was negative, it was set to zero before computing the mole fractions. Combinations of temperature and water content, at which no measurement was done, are marked by **0**.
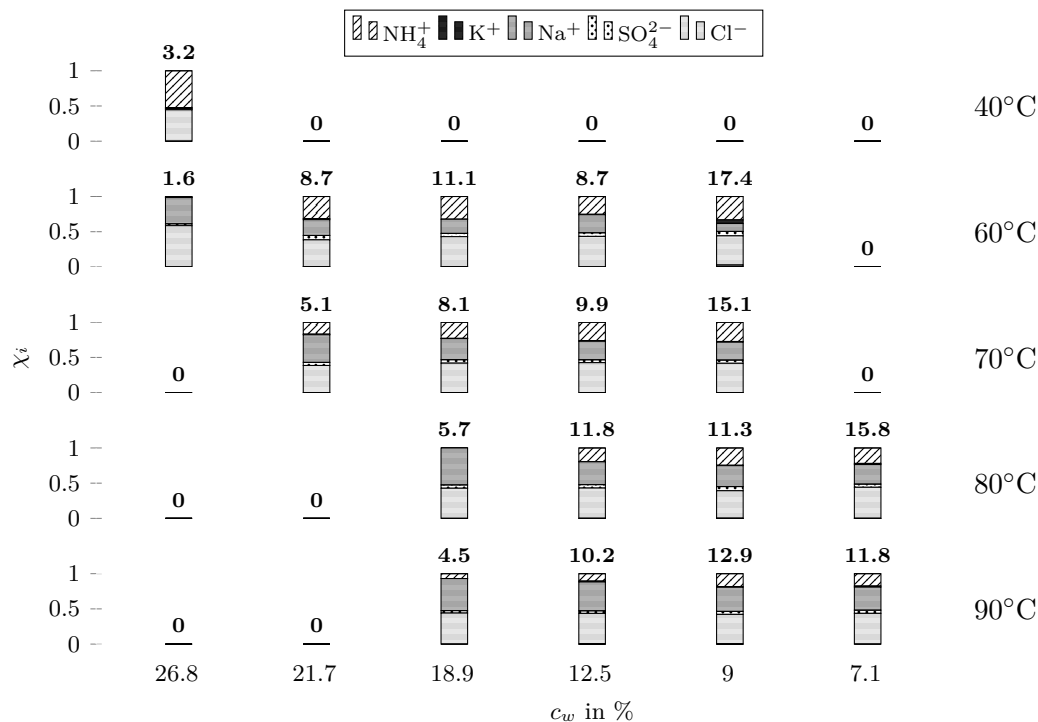
3.2. Solution

Estimated equilibrium molalities of ions in the solution are given in **Tab. 2**. The ionic strengths were computed to values ranging between 36 and about $200\,\mathrm{mol/kg}\,H_2O$. The uncertainty of the estimated ionic strength values can be seen from the 10 and 90 % quantiles from MCA. The relative uncertainty range for the single ion molalities is comparable. The major part of the ionic strength is associated with NH_4NO_3. When comparing the molalities of NO_3^- and NH_4^+, it is apparent that values for NO_3^- are also above those for NH_4^+, which is due to the formation of solid NH_4Cl. Molalities at equal water contents and increading temperatures, e.g. $c_w = 18.9\,\%$, show relatively small increase. Decreasing water contents led to relatively large increases of the molalities. Therefore, the influence of water content on ion concentrations seems to be dominant compared to increased temperatures.

The comparison with solubilities of single salts (**Tab. 3**) shows that at the highest concentrations, the estimated ion solubilities reach or even exceed solubilities for the most soluble single salts containing the respective ion. Na^+ and Cl^- show up to about double the solubility as would be expected from the single salt solubilities.

Tab. 2: Estimated equilibrium molalities of solutions at different temperatures T and initial water contents c_w. The estimated distribution of the ionic strength I is given as the 10 and 90 % quantiles estimated from MCA. For the ions, only the median values are given for better display.

T	c_w	I_{q10}	I_{q90}	NH_4^+	NO_3^-	PO_4^-	Cl^-	SO_4^{2-}	Na^+	K^+
°C	%					mol/kg H_2O				
40	26.8	36.2	46.6	19.9	21.4	1.5	7.6	1.4	8.9	5.1
60	26.8	36.8	47.2	20.2	20.6	1.5	9.4	1.4	9.8	4.8
60	21.7	47.9	58.7	25.8	28.3	2.0	10.3	1.5	11.4	6.6
60	18.9	56.1	68.6	29.7	33.7	2.4	10.5	1.7	13.2	8.0
60	12.5	89.3	109.4	48.5	53.2	3.9	17.3	2.7	20.4	12.6
60	9.0	120.5	147.8	69.0	79.2	4.2	19.4	2.7	33.6	16.8
70	21.7	47.9	57.0	26.4	27.5	1.9	10.4	1.5	10.4	6.5
70	18.9	57.1	66.7	30.8	33.0	2.4	11.1	1.8	12.2	7.8
70	12.5	85.1	101.3	46.0	51.5	3.6	15.3	2.7	18.2	11.9
70	9.0	123.1	150.7	65.8	78.9	6.0	18.1	3.5	24.0	17.8
80	18.9	57.8	70.6	33.5	32.9	2.3	12.6	1.7	12.5	8.2
80	12.5	90.5	110.8	51.8	54.8	4.0	15.7	2.5	18.0	13.2
80	9.0	122.6	150.0	67.2	75.6	5.3	24.1	3.2	26.6	17.6
80	7.1	160.4	195.7	89.7	100.2	7.7	23.0	4.3	31.7	23.0
90	18.9	59.0	70.2	32.6	33.1	2.3	13.2	2.1	12.9	7.9
90	12.5	93.4	110.9	53.2	55.9	3.9	17.0	3.0	17.6	13.0
90	9.0	129.9	154.6	72.1	78.9	5.8	21.7	3.8	24.0	19.0
90	7.1	166.9	203.4	93.9	102.0	7.2	29.8	5.0	33.7	23.7

Tab. 3: Equilibrium molalities of single salt solutions from literature for some of the temperatures investigated in this work (Lide, 2009)

T	NH_4Cl	Na_2SO_4	NH_4NO_3	Na_2HPO_4	$NaCl$	KCl	$NaNO_3$	KNO_3
°C				mol/kg H_2O				
40	8.6	3.4	36.1	3.8	6.3	5.8	12.2	6.2
60	10.3	3.1	52.6	5.8	6.4	6.1	14.6	10.8
90	13.2	3.0	93.4	7.5	6.7	7.2	19.0	20.4

3.3. Reaching the equilibrium

At the thermodynamic equilibrium of an electrolyte system, the Gibbs energy, ΔG, is at the minimum. Due to the kinetics of crystallization and initial formation of seeds, an electrolyte system may be at an equilibrium other than the thermonadynamic equilibrium, which can be called the kinetic equilibrium. Theses kinetics are associated with solid liquid equilibria proceeding to the solid side and play therefore mainly a role in the process of crystallization. In order to estimate, if the thermodynamic equilibrium is reached and after which time, the equilibria found by crystallization and dissolution can be compared.

Therefore, two time series experiments were initially conducted for two water contents at a temperature of $70°C$ as crystallization and dissolution, respectively. The respective results are displayed in **Fig. 8**. In both crystallization experiments, initially only NaCl was present and only at $30\,h$ and later, increasing amounts of NH_4^+ and SO_4^{2-} were observed. As expected, the total masses of solids increased over time for crystallization and generally decreased for dissolution. The results of the first experiment (**Fig. 8(a)**) showed very little variation for dissolution. Compositions of the solids for crystallization and dissolution were different after an equilibration time of $55\,h$. In the second experiment (**Fig. 8(b)**), a trend for NH_4^+ was observed in the opposite direction for dissolution compared to crystallization.

In both experiments, after 55 and $145\,h$, respectively, no equal composition of the solid phases for crystallization and dissolution were observed. Additionally, in the second experiment the solids composition during dissolution was not found to be constant even after $80\,h$. Therefore, it was concluded that the thermodynamic equilibrium was not yet reached.
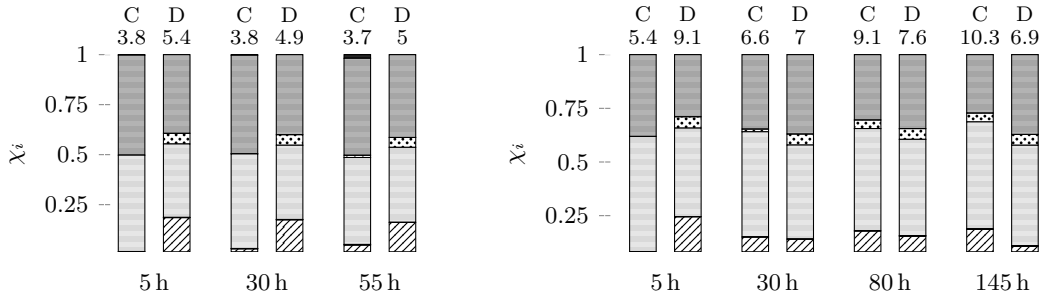
(a) Crystallization and dissolution at $c_w = 21.7\,\%$ and $T = 70°C$

(b) Crystallization and dissolution at $c_w = 18.9\,\%$ and $T = 70°C$

Fig. 8: Plots of two sets of timeseries of crystallization and dissolution experiments. The species are from bottom to top ⬚⬚ NH_4^+, ⬚⬚ Cl^-, ⬚⬚ SO_4^{2-}, ⬚⬚ Na^+ and ■■ K^+. The left bar at each time represents crystallization (C), the right bar dissolution (D). Values above the bars indicate the total mass of solids m_{tot}^s in g, for which the standard deviation was found to be around $\pm20\,\%$ (see also section 3.5.1).

3.4. Full nitrification

Besides partially nitrified urine, as it was observed in the effluent of the nitrification reactor by Udert and Wächter (2011) without addition of any chemicals, fully nitrified urine was investigated. Under the assumption, that two mole of alkalinity need to be provided per mole NH_4^+ oxidized to NO_3^- according to equation (1), two hypothetical compositions for fully nitrified urine using NaOH and $CaCO_3$ were computed. The compositions as given in **Tab. 1** on page 8 were used, with the only modification to set carbonate to zero. In distillation experiments the stripping of all carbonate as CO_2 was confirmed (Udert and Wächter, 2011).

Preliminary solubility experiments were performed for the option with NaOH addition. For a comparison between partial and full nitrification with regard to highest NaCl removal achieved, see **Tab. 4**. The prior simulation using EQ3/6 with Pitzer equations (Wolery and Russell, 2003) predicted first crystallization at a 18.4 fold concentration ($c_w = 50.0\%$) at room temperature, where for the partially nitrified urine, the same prediction gave a 35.7 fold concentration ($c_w = 47.4\%$). For both cases, synthesizing the respective solution confirmed these predictions. The initial water content for fully nitrified urine was 94.9% (96.9% for partial nitrification). Experiments with water contents of 41.2% at 25 and $40°C$ and 28.7% at 40 and $70°C$ were done. For the lower concentration, only sodium and nitrate with a minor amount of sulfate was observed in solids and only for the higher concentration, additionally some Cl^- was present as shown in **Tab. 4**.

Tab. 4: Comparison of partial and full nitrification using NaOH for balancing alkalinity consumption during nitrification

Content of species	Partial nitrification		Full nitrification NaOH	
	value m-%	condition $c_w/\%$, $T/°C$	value m-%	condition $c_w/\%$, $T/°C$
initial N	21.8	-	12.8	-
initial Cl^-	12.6	-	7.4	-
initial Na^+	8.2	-	25.8	-
maximal N loss	11.3*	7.1 / 80	73.5**	28.7 / 40
maximal Cl^- removal	49.3	7.1 / 80	61.0	28.7 / 70
maximal Na^+ removal	32.5	7.1 / 90	67.0	28.7 / 40
final N	23.5-24.1	-	12.4 − 13.6	-
lowest final Cl^-	7.1	7.1 / 80	6.4	28.7 / 40
lowest final Na^+	6.0	9.0 / 90	24.3	28.7 / 70

* as NH_4, higher losses up to 17.4% observed for T=$60°C$

** as NO_3

3.5. Statistical analysis

3.5.1. Error analysis

The distributions of the errors ε_i for all ions and water and the variation of mass of total solids can be found in **Fig. 9**. The residuals were found to follow normal distributions well. The statistics used for Monte-Carlo analysis can be found in **Tab. 5**.

Prior to equilibration experiments, solutions of the single salts used in this work were given to chemical analysis and deviations of below $\pm 1.5\,\%$ (up to $\pm 5\,\%$ for NH_4^+ and NO_3^-) were found (data not shown). The deviations of the mass balances ε_i were found to be in average $2.5 \pm 5.5\,\%$ ($0.7 \pm 5.2\,\%$ excluding K^+). The mean value of this error range is comparable to the error related to chemical analysis and the larger deviation is associated to the error of the over all experimental method.

The deviation of K^+ was found to be related to the chemical analysis of the residue using IC. Measuring six samples of the residue again using inductively coupled plasma (ICP) analysis, values for the concentration of K^+ were between 18 and $33\,\%$ higher compared to the measurements using IC. Deviations between IC and ICP analysis for samples of the mother solution were less than $5\,\%$ (data not shown). Based on these findings the measured amounts of K in the residue samples were corrected (see Appendix A.2).
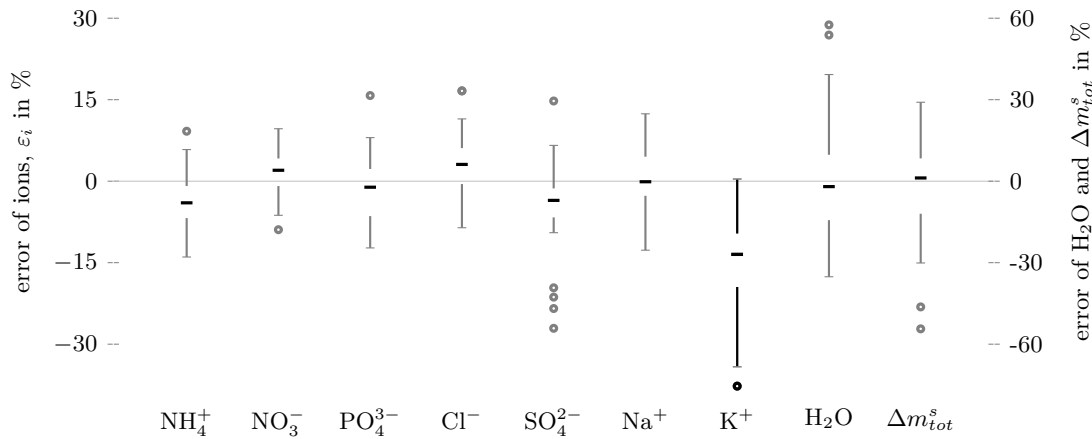

Fig. 9: Whisker plots of distributions of errors of mass balances of ions, H_2O and the variation of the total mass of solids; The whisker plots indicate the median as the horizontal bar, the first and third quartile as the inner ends and the approximate $95\,\%$ prediction interval as the outer ends of the whiskers. Outliers are indicated as dots, if they exceed the interquartile range by more than 1.5 times. The whisker plots of the seven ions refer to the left y axis, those of H_2O and Δm_{tot}^s to the right y axis. Since the amount of water can only be determined indirectly by subtracting the mass of the sum of ions from the total mass of the sample, single ion errors accumulated in this quantity. The original distribution of K^+ with the systematic deviation as shown in this graph was corrected.

Tab. 5: Statistics of error distributions given as the average $\bar{\varepsilon}_i$ and standard deviation sd. For Monte-Carlo analysis, normal distributions as $\mathcal{N}(\mu_i = \bar{\varepsilon}_i, \sigma_i = sd)$ were used for each ion i. Measurements of ions in liquor and residue were corrected for bias using μ_i.

Statistic	NH_4^+	NO_3^-	PO_4^-	Cl^-	SO_4^{2-}	Na^+	K^{+*}	H_2O	Δm_{ions}^s	total mass
$\bar{\varepsilon}_i$ in %	-3.5	1.7	-1.9	2.3	-4.0	1.0	-13.8 / -5.0	1.3	1	-1.1
sd in %	4.6	4.0	5.9	4.9	6.5	5.3	7.9 / 4.4	20.5	17.9	1.9

* For K, the original and the corrected distribution is given. The procedure of the correction is described in section A.2.

3.5.2. Comparison of methods for estimation of solids

Since initially, it was not clear which method for the evaluation of the experiments would give a "truer" result, using the water content or the amount of NO_3^- instead, both methods were applied (refer to section 2.2 for details about the methods). The results of this comparison are summarized in **Tab. 6**. The method using NO_3^- yielded clearly much lower error ranges compared to the analysis using the water content for both, mass balances and charge balances. This is conclusive when comparing the error ranges of NO_3^- and H_2O in **Fig. 9**. From the analysis using the water content method, it could be seen that within the error range of the method, the amount of nitrate in the solids was zero, which was the underlying assumption for using NO_3^- as quasi solvent. As the result of the comparison, the NO_3^- method was employed for the calculations of all final results presented.

3.5.3. Separation of solution and solids

The extend of separation of mother liquor and residue was dependent on the amount of solids precipitating and consequently on the experimental conditions (given by c_w and T). Between 12 % and 61 % of the initial total composition remained as residue after removing the mother liquor. The correlations of the water content of the residue and

Tab. 6: Comparison of evaluation of experiments with the two methods using the estimated water content and using NO_3^- as a quasi solvent; For summarizing the results of the Monte-Carlo Analysis, the mean and the range of the 80 % confidence interval (CI_{80}) of all ions in all experiments is given. For summarizing the charge balances, the mean μ and the standard deviation σ of all ions in all experiments are given.

Analysis	Statistic	Method	
		water content	NO_3^- as reference species
mass balance	CI_{80} min in %	0.1	0.2
	CI_{80} mean in %	9.1	2.4
	CI_{80} max in %	50.5	7.3
charge balance	μ of deviation in %	-46.7	-1.1
	σ of deviation in %	15.5	8.1

the proportion of the sum of ions from the liquid phase present in the residue against the mass of the dry residue are depicted in **Fig. 10**. The relative water content in the residue decreased with increasing mass of the dry residue, which was probably an effect of the smaller water content at higher concentrations (**Fig. 10(a)**). The proportion of ions from the liquid phase in the residue, however, was rather constant (**Fig. 10(b)**). The maximal percentage of ions from the liquid phase was around 80 % of the total residue mass, which refers to 58 % of the sum of ions in the liquid phase.
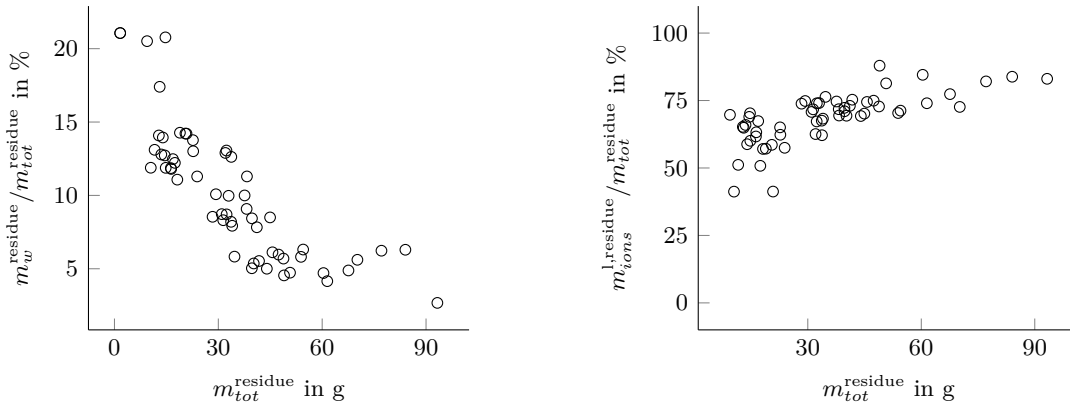
(a) Water content of residue plotted against the mass of dry residue

(b) Percentage of ions from solution in the dry residue plotted against the mass of dry residue

Fig. 10: Correlation of water content (a) and proportion of liquids in residue (b) against total mass of dry residue. The water content of the residue increases strongly for very small amounts of residue and levels off at around 5 % for large amounts of residue. The percentage of solids from solution in the residue is relatively constant between about 50 and 80 %. $N = 57$ data points are displayed.

4. Discussion

4.1. Feasibility of experimental method

The experimental method used in this work is rather simple. Information from mother liquor and residue was used, although only liquor composition would be sufficient to estimate solids. Determining liquor and residue composition, however, enhances accuracy of results and allows for the assessment of the quality of the data obtained using mass balances (see section 3.5.1 on page 18). Considering the complexity of the system, the average deviations of the mass balances as well of the charge balances show a good accuracy of the analysis and suggest, that reliable conclusion can be drawn from the data.

During extraction of mother solution, the focus was put on maximizing the separation of solution and residue. Nevertheless, around 70 % or more of the solids in the dried residue were estimated to be contamination from solution. For repeated experiments at the same conditions and the same equilibration time, a relatively big variation of the sum of solids was found. The average deviation from the mean within one experimental condition had a standard deviation of 17.9 %. This variation was taken into account in the Monte-Carlo analysis (section 3.5.1 on page 18).

For the results presented here, this means that the percentage of removal is rather underestimated. With an improved experimental procedure, higher removal for all solids is expected. This also needs to be taken into account for the interpretation of the molalities of the solution (section 3.2), which can be expected to be overestimated by the amount, which was removed as solids. In an upscaled application, however, optimal separation will be achieved neither, and therefore the presented results might just give a good estimate for the amount of solids removal, that can actually be expected.

Based on these findings, the focus during extraction of solution should be put on removing as little solid crystals as possible. This could be done by keeping the needle tip always at a level, where mainly pure solution is present. Even if the solution contamination in the residue might go up to 90 % or higher, the accuracy of the estimation of solids should be enhanced.

4.1.1. Reaching the equilibrium

As described in section 3.3 on page 17, results of the initial equilibrium evaluation comparing time series for crystallization and dissolution were unequivocal. Therefore, in later experiments one sample was always equilibrated at least double as long as the parallelly run samples, in order to get an indication, if the thermodynamic equilibrium was reached. Equilibration times between 60 and 100 h were chosen for the experiments. For the design of a NaCl removal process, equilibration times of less than 24 h might be feasible, longer times are not relevant for large scale application.

Under some experimental conditions, a different phase composition was observed for the later sampled solution (see appendix A.3 on page 33). The implication of these observations is, that solid phases obtained in crystallization experiments by cooling or

distillation at comparable equilibration times might look very different to those found here.

4.1.2. Crystallization kinetics

For both crystallization and dissolution experiments, kinetics of solid liquid equilibrium reactions were observed. In the preliminary experiments depicted in **Fig. 8** on page 17, a slow formation of both Na_2SO_4 and NH_4Cl was observed during crystallization. For the dissolution experiment at the lower water content, NH_4Cl appeared to dissolve increasingly over time. For the crystallization experiment at the same conditions, more NH_4Cl crystals formed over time.

In some later experiments, where one sample was kept about double the time in the oil bath than the replicates, differing solid compositions were found for the different equilibration times. In one case, the portion of NaCl increased, in another case this happened similarly for NH_4Cl. Since only one sample was available for these observations, the deviations might also come from random experimental errors.

In a multicomponent system like the one investigated here, kinetics of the interplaying equilibrium reactions seem to play an important role. In the equilibration process, one component, e.g. NaCl, might dissolve thereby promoting the crystallization of another salt, e.g. NH_4Cl. The rate of NH_4Cl crystal formation will in this case be limiting to the dissolution of NaCl.

4.1.3. Determining solid phases

Determining identities of solid phases can only be done indirectly by finding a likely combination of solid salts for the composition of ions. With regard to the identity of solid phases, which were deduced from the mole fractions of the solids (**Fig. 7** on page 15), mainly NaCl, Na_2SO_4 and NH_4Cl were present. Additionally, solid $NaK_3(SO_4)_2$ (Glaserite) was suggested by simulations and might have been present, where K^+ was detected in the solids. Based on the small amount of K^+ found as solid, however, the amount of Glaserite is probably very small.

The method was limited in the way that solid phases could only be estimated from the ion composition of the computed solids. The presence of double salts or hydrates cannot be determined directly. Frequently, x-ray diffraction (XRD) is employed to determine identities of solid crystals. This method was not employed since contamination of the residue with mother solution was as high as 70 %, which is likely to prevent distinguishing the actual solid phases from those formed by the solution in the residue during drying.

4.1.4. Effect of pH

pH values of nitrified urine are between 6 and 7. At increasing concentrations of the nitrified urine, pH is assumed to decrease as NH_4NO_3 is the main component of the solution and NH_4^+ acts as a weak acid. A Simulation using EQ3/6 with Pitzer equations gave a pH of 4.5 for the synthetic, 35 fold concentrated solution. Looking at the pH

measurements of the diluted extracted solution plotted against the measured electric conductivity confirmed, that pH decreases with increasing concentration (**Fig. 11**).

pH dependent species in the investigated system were ammonium, sulfate and phosphate. For phosphates, solubility is decreased at high pH, which is used e.g. for struvite precipitation in stored urine. Therefore, at the low pH, no phosphate precipitation was observed. Hydrogen sulfate (HSO_4^-) is only present in relevant amounts relative to SO_4^{2-} at very low pH (e.g. 10% HSO_4^- at pH = 2.9). The ammonium-ammonia equilibrium is shifted very much to the NH_4^+ side at the present pH levels (about $1800/1 : NH_4^+/NH_3$ at pH = 6). Increased pH should favor NaCl crystallization, since less ammonium for NH_4Cl formation is present. However, losses of nitrogen by ammonia volatilization might occur.

4.1.5. Review of other experimental methods

Besides the direct method like the one used here, synthetic and isopiestic method exist, which allow for determining the occurance of phase transitions and might therefore be applicable to investigate the phase behavior of a system in more dimensions, i.e. in addition to temperature and water content also for varying compositions.

The idea behind the synthetic method is to use the information of the initial overall composition and change one system parameter, e.g. temperature, water content or composition. By monitoring one property of the system, e.g. electric conductivity, the plot of this property against the system parameter can give information of phase changes in the form of sharp bends. The solid phase composition is determined by additional chemical analysis (Bousmina et al., 2003; Khlissa et al., 2004).
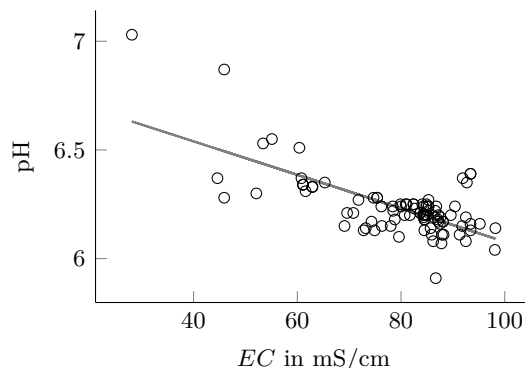

Fig. 11: Correlation of pH against electric conductivity EC in extracted solution for all experiments conducted; The pH significantly decreases with increasing electric conductivity, i.e. with increasing concentration of mother solution. Since the mother solution was diluted between 11 and 21 times (mass H_2O to mass solution), this suggests that the pH of the mother solution might well be around or below 4.5. The temperatures of pH and conductivity measurements ranged between 20 and 24.1°C and 21.4 and 24.8°C, respectively. Statistical analysis of the linear regression: $p = 3 \cdot 10^{-15}$, $R^2 = 0.49$, $N = 97$.

The isopiestic or isotonic method captivates by its beautiful simplicity (Platford, 1972; Scatchard et al., 1938). The method is based on the idea of the equilibration of several unsaturated samples of known composition, which are kept under the same atmosphere as a saturated control solution with large excess of solids. Since the solvent activity of the samples is larger than that of the control solution, solvent distills from the unsaturated samples until the chemical potential of the solvent of the sample and the control solution are equal.

A very valuable source of information for designing solubility experiments is given by Cohen-Adad and Cohen-Adad (2004).

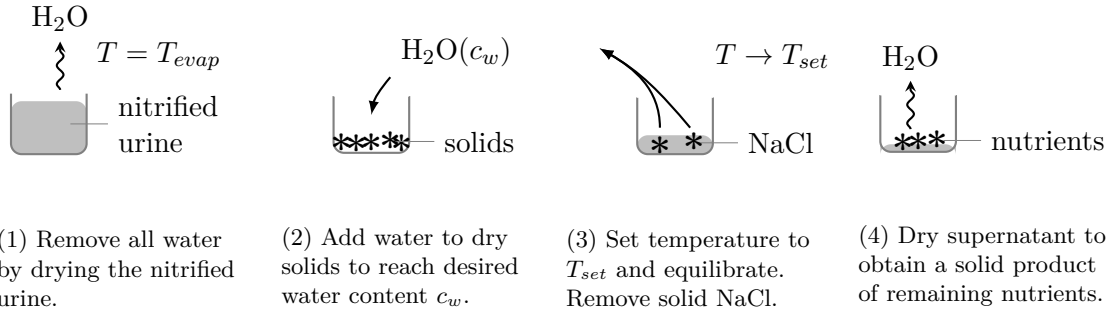## 4.2. Extend of sodium chloride removal

Results of the solubility experiments in this work show that selective removal of NaCl from nitrified urine at elevated temperatures is possible. The extend of sodium and chloride removal was at most 33 and 50 %, respectively (**Fig. 5** on page 13). The loss of nitrogen as NH_4^+ was relatively small with 10 %, the other important nutrients K and P were almost fully retained. SO_4^{2-} loss was around one third, but sulphate is not the compound of main interest with respect to the nutrient recovery.
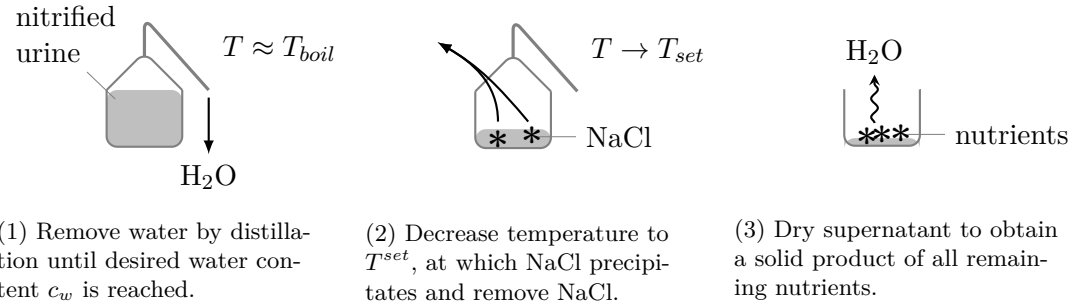
4.2.1. Ammonium nitrate decomposition

Based on the results for highest removal conditions, the Cl^- content of the final solid product would be still at around 7 % per mass. The NH_4NO_3 content would at the same time be around 24 %. The regulatory requirement for fertilizers in the EU state a chloride content of below 0.02 % for products with an NH_4NO_3 content of more than 28 % (European Parliament and European Council, 2003). Since the NH_4NO_3 content is not too far below this limit and nitrogen contents in urine are subject to strong variability, the addition of fillers like $CaCO_3$ to the product as suggested by Udert and Wächter (2011) might be needed for meeting legal requirements and guaranteeing product safety.

4.2.2. Salinity and sodicity

As described in section 1.2.2, both sodium and chloride bear the potential to counteract the enhancing effect of a fertilizer on plant growth. The observed reduction in both sodium and chloride content might have a remarkable impact. However, no reliable data is available on this issue to date. Quantitative estimations of the impact of a given amount of salt added to a soil are necessary in order to assess the potential implications of urine fertilizer on soil salinity. An in depth literature review on salt concentration in irrigation water and observed effect on salinity might give further insight to the issue. Additionally, the salinity modeling program UNSATCHEM might be applicable for quantifying salinity increase due to NaCl addition (Suarez, 1997).

(a) Hot dissolution

(1) Remove all water by drying the nitrified urine.	(2) Add water to dry solids to reach desired water content c_w.	(3) Set temperature to T_{set} and equilibrate. Remove solid NaCl.	(4) Dry supernatant to obtain a solid product of remaining nutrients.

(b) Distillation

(1) Remove water by distillation until desired water content c_w is reached.	(2) Decrease temperature to T^{set}, at which NaCl precipitates and remove NaCl.	(3) Dry supernatant to obtain a solid product of all remaining nutrients.

Fig. 12: Process application for NaCl removal prior to full nutrient recovery from nitrified urine using (a) hot dissolution and (b) distillation

4.3. Process application and alternative processes

The results of this work could be applied to the removal of NaCl from real nitrified urine using hot dissolution or distillation. The process steps required for each of the two methods are illustrated in **Fig. 12**.

Hot dissolution is equivalent to the method employed for solubility experiments in that both methods are based on dissolving the salts. Therefore, reasonable agreement between laboratory and scaleup results with regard to the amounts and identities of solids should be given. Besides conventional industrial drying processes, solar thermal energy could be employed for the initial drying step. This would be an economical alternative and enhance the energy balance for the process.

Distillation would require one process step less, however it requires more careful process monitoring. In the concentration range investigated here, the elevation of the boiling point of an electrolyte solution with increasing ionic strength becomes relevant. Udert and Wächter (2011) determined the boiling point to be at 130°C, when 99.5 % of the water had been removed by distillation. The boiling point elevation follows an exponential curve starting from around 98 %. The highest salt concentration with a water content of 7.1 % in this study is equivalent to a removal of 99.76 % H_2O, which significantly increases energy consumption for distillation.

4.3.1. Full nitrification

One of the major strengths of the partial nitrification process developed by Udert et al. (2003a) is that it does not require any addition of chemicals. Nevertheless, for the reasons stated below, it might be beneficial to consider full nitrification even if it requires chemicals.

One advantage of fully nitrified urine is that it does not contain NH_4NO_3 and therefore, its decomposition is not a potential hazard. Investigations are required, however, on whether there is a significant difference in nitrogen plant availability, if it is supplied in form of NO_3^- or NH_4^+. Since $NaNO_3$ is a commonly used fertilizer, this might be not a very relevant issue. Additionally longer retention times required by full nitrification should be taken into consideration.

With respect to removal of NaCl, results of the preliminary investigation of fully nitrified urine using NaOH (**Tab. 4** on page 18) were not very promising. Since $NaNO_3$ is present at very high concentrations compared to NaCl and other components, it was observed as the primary component in the solids obtained in the experiments. Only when accepting losses of nitrogen of almost three quarters, significant amounts of NaCl could be removed. Selective NaCl removal similar to the one shown for the partial system seems therefore not feasible. Though results show a slightly smaller final percentage of Cl^- per mass compared to the composition for partial nitrification, this is due to the relatively large added amounts of NaOH. For partial nitrification, the same effect could be achieved by simply adding more economic fillers. The Na^+ percentage before and after crystallization is three and four fold higher for the NaOH process, respectively. With regard to sodicity problems associated with high sodium contents of the product (section 1.2.2), this might be undesired.

Further investigations on full nitrification by addition of $CaCO_3$ should be done. Carbonate represents a lower cost option. The low solubilities of calcium carbonates and phosphates might limit the selective removal of NaCl. Struvite precipitation prior to nitrification could be employed to maximize the recovery of phosphate.

4.3.2. Fractional crystallization

In order to increase the extend of chloride removal, fractional crystallization could be employed. The idea of fractional crystallization is to cycle the crystallization of fractions of two components of the system, e.g. NaCl and NH_4Cl, by altering temperature and water content of the system. An illustrated example for a three component system can be found in appendix A.4. Since the relative composition of the ions in the system changes during fractional crystallization, a more complete knowledge of the phase behavior of the system might be required compared to a one step crystallization (evaporative crystallization). In some cases, considering only relevant subsystems might already facilitate the design of fractional crystallization with reasonable accuracy. These subsystems with less interacting components are easier to handle compared to the more complex overall system.

From the results obtained here, a preliminary fractional crystallization process could

be designed. A phase transition was observed from NH_4Cl at 40°C to NaCl at 60°C, at a water content of 26.8 % (**Fig. 7** on page 15). Alternating between these two temperatures might allow for selective removal of Cl^- as NaCl as well as NH_4Cl.

4.4. Feasibility of numerical simulation

For rationalizing the experimentally obtained solubility results, the Pitzer and the extended Uniquac model were applied. Both models, however, were only able to give rough reference points for the concentration, at which crystallization might start and which solid phases might be likely to form. The extended Uniquac model for example is only based on binary interactions parameters, i.e. only two ions interact with each other at a time. Therefore, the application to a system containing seven ions represents a large extrapolation.

Typically, at most five component systems are simulated, for which deviations of predictions for solid phases are rather large. In a comparison of different models including the extended Uniquac model, Lin et al. (2010) stated: "It was found that the calculation of solid-liquid equilibria in multi component electrolyte solutions is a very difficult task."

Improvements on the capabilities of the models might be possible by closing gaps in the solubility data available for parametrization. For the extended Uniquac model, these gaps were identified for some subsystems relevant to the urine solution (see appendix A.5, **Tab. 7** on page 35).

Although model application was not successful for the present system, the solubility data obtained in this work could be employed to develop models further, as it represents a high ionic strength multi component electrolyte system. There is not much comparable data in the literature.

5. Conclusions

Solubility experiments with synthetic nitrified urine in the temperature range from 40 to 90° were conducted. The initial hypothesis that Cl^- can be selectively removed from this solution as NaCl at elevated temperatures could be confirmed.

The maximal removal achieved was about 33 % for sodium and 50 % for chloride with relatively little loss of nitrogen and no loss of phosphorous or potassium. This extend of removal is probably not sufficient to lower the risk associated to the catalytic effect of Cl^- on NH_4NO_3 decomposition. The remaining amount of Cl^- at the highest removal was still around 7 % by mass. However, with regard to potential soil salinization from urine fertilizer use, the observed removal of NaCl might have a measurable effect. The content of sodium in the final product might be similarly relevant to its fertilizing properties as that of chloride.

It was also found, that the thermodynamic equilibrium of the urine solution is probably only reached after equilibration times of much longer than 100 h, especially at high concentrations. For process application, however, only much shorter equilibration times of less than 48 h are relevant and the data obtained in this work will be a good source for planning and design of NaCl removal processes from urine.

6. Outlook

To verify the applicability of the results obtained in this work, comparable experiments with real nitrified urine should be done. In real nitrified urine there are some organic compounds present, which might affect crystallization of inorganic salts. The percentage of TOC is, however, below 0.5 %, and should therefore not have a significant effect. An interesting experimental setup would be to use dried residue of real nitrified urine together with hot dissolution and assess the removal of NaCl. This method would be equivalent to the solubility experiments performed in this work. Alternatively, distillation experiments could be conducted. However, since this approach would represent the process of evaporative crystallization, this method is not necessarily appropriate for verifying the applicability of the results obtained in this work. It is likely that no sulfates and less ammonium will be observed in the solid phase due to slow reaction kinetics.

Generally, nutrient concentrations in urine vary widely depending on climate, diet and other parameters (Schouw et al., 2002). Despite these variations, losses of nitrogen during collection and storage can decrease nitrogen content by 50 % and more. N content in fresh urine is reported to be at levels as high as 9200 mg/l (Udert et al., 2006). N levels in the effluent of the lab scale nitrification reactor as described in Udert and Wächter (2011) were around 2400 mg/l. Therefore, investigations on the effect of varying nitrogen concentrations on NaCl removal would be of interest in order to be able to apply the process to a wide range of settings. Additionally, mechanisms causing nitrogen losses need further investigation. These losses need to be controlled in order to maximize recovery of valuable nutrients.

As discussed earlier, full nitrification of urine might be beneficial in that the complete oxidation of ammonium to nitrate bypasses the dangers associated with ammonium nitrate containing products. Drawbacks of full nitrification would be the longer residence time required and the need for addition of chemicals to balance the alkalinity consumption. Further investigations are necessary regarding the process of full nitrification itself as well as the properties of the resulting solution with regard to NaCl removal.

To date, little knowledge is available on the impact of the amount of sodium chloride on soil salinity and plant growth. Especially quantitative data is missing. Therefore, further investigations are necessary for determining the effect of different NaCl contents in urine fertilizer in order to estimate the required removal.

Modeling of multicomponent systems at high ionic strength is a difficult task. Parametrization of existing models with subsystems at relevant temperatures might improve their capabilities. This will require the creation of additional experimental data. The further development of numerical models will be a task for the experts in this field and cannot be done by those who would like to apply a model to their specific problem.

For future work on nutrient recovery from urine, I would like to state the need for collaboration of various disciplines. The combined efforts of environmental and process engineers, chemists, plant biologists and soil scientists will be required to overcome limitations of production and application.

Acknowledgment

A. Appendix

A.1. Documentation of digital resources

During this diploma thesis, many digital resources accumulated. These are e.g. the experimental raw data in digital form and the R scripts used for evaluation of the experiments. In order to ensure their safe storage and future access, copies are stored in a folder on the Eawag servers. The folder contains a file `readme.txt`, which describes the files contained.

A.2. Analysis of deviation of measurements of K^+

As discussed in section 3.5 on page 18, the measurements of K^+ significantly underestimated the amount of K^+ additionally added. For no other ion a similar deviation was found. When looking at the correlation of the deviation of K^+ and the analyses of the samples residue, ε_{K+} was significantly larger the larger the portion of the total amount of K in the residue was, i.e. $m_K^{tot}/m_{K+}^{residue}$ (**Fig. 13(a)**. Additional K measurements of six samples using inductively coupled plasma (ICP) gave 18 to 34 % increased concentrations compared to the measurements using IC (data not shown). The regression depicted in **Fig. 13(a)** suggests an underestimation of the K concentrations in the residue of 97 %. The reasons for the measurement error for only K and only in the residue were unknown
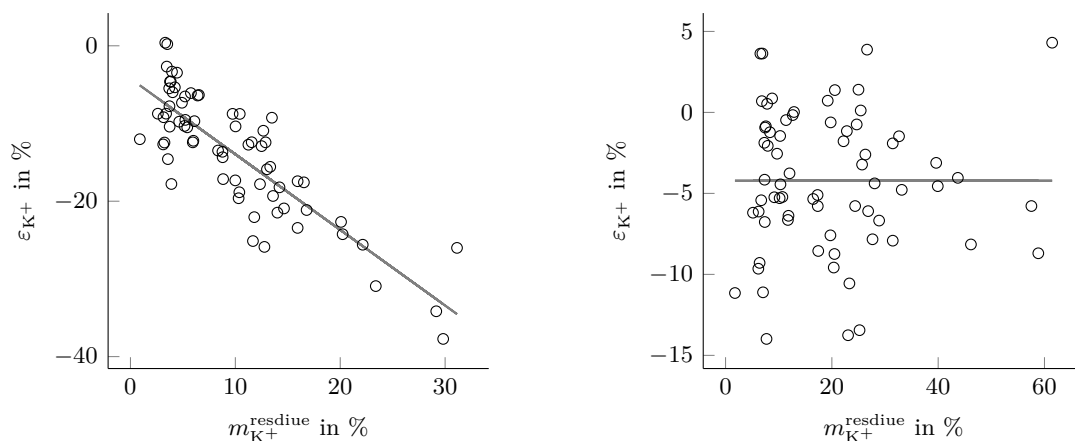
(a) Initial correlation of the mass balance errors of K against the percentage of K^+ in residue; Statistics: $m = -0.97$, $p \leq 2 \cdot 10^{-16}$, $R^2 = 0.70$; The distribution of the error of K^+ in % was $\mathcal{N}(\mu = 13.8, \sigma = 7.9)$.

(b) Correlation after correction; Statistics: $m = 2 \cdot 10^{-17}$, $p = 1$, $R^2 = 3 \cdot 10^{-32}$; The distribution of the error of K^+ in % was $\mathcal{N}(\mu = -5.0, \sigma = 4.4)$.

Fig. 13: Correction of biased measurement of K^+ in residue samples; The measurements of K in the residue deviated significantly (a). After correction of the measured K values of the residue using the regression $m = -0.97$, the error of K was distributed much like those of the other ions (b).

to this point and need further investigations. In order to be able to estimate the presence of K in the solids, residue K measurements where corrected using the slope m and axis intersection c in the following manner:

$$m_{K+}^{residual,corrected} = m_{K+}^{residual} \cdot (1 - m) - m_K^{tot} \cdot c/100 \tag{18}$$

The resulting distributions of the mass balance errors was then comparable to those observed for the other ions (**Fig. 13(b)**). For all other ions, $p > 0.017$, $R^2 < 0.1$ and slope $m < \pm 0.1$ (largest for Na^+, generally cations showed slightly stronger tendency for such a correlation)

A.3. Equilibrium

Due to the findings in the initial time series experiments (section 3.3 on page 17), one replicate at each combination of experimental conditions was equilibrated longer than the others. In a few cases, it was found that the sample, which was equilibrated longer than the others, shows a different composition of the solids compared to the other samples. The composition of the solid phases of two experiments are displayed in **Fig. 14**. In one experiment (**Fig. 14(a)**), it was found that the mole fraction of NH_4^+ decreased from 0.28 to 0.18, in another experiment (**Fig. 14(b)**), the mole fraction increased from 0 to 0.23. These findings cannot yet be explained and need further investigation.

A.4. Principle of fractional crystallization

Fractional crystallization can be employed to separate solids in an electrolyte solution. The principle for a simple three component system with two salts in water is illustrated in **Fig. 15** on page 34. The basic ideas is to alternatingly remove one of the components by changing water content and temperature of the system.

(a) Experiment with three duplicates at $c_w = 12.5\%$ and $T = 60°C$

(b) Experiment with four duplicates at $c_w = 18.9\%$ and $T = 90°C$

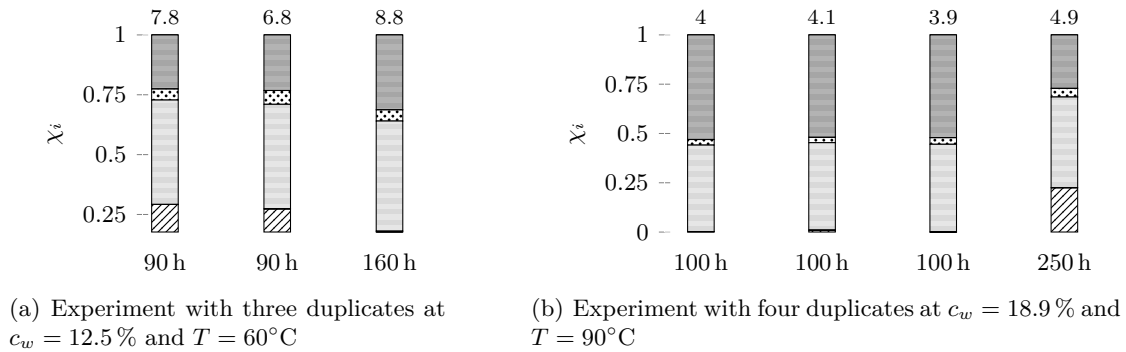**Fig. 14**: Plots of two sets of experiments with different equilibration times. For both experiments, the sample, which was equilibrated longer than the others, shows a different composition of the solids. The species are from bottom to top ▨▨ NH_4^+, ▨▨ Cl^-, ▨▨ SO_4^{2-} and ▨▨ Na^+. Values below the bars indicate the equilibration time, values above the bars indicate the total mass of solids m_{tot}^s in g.
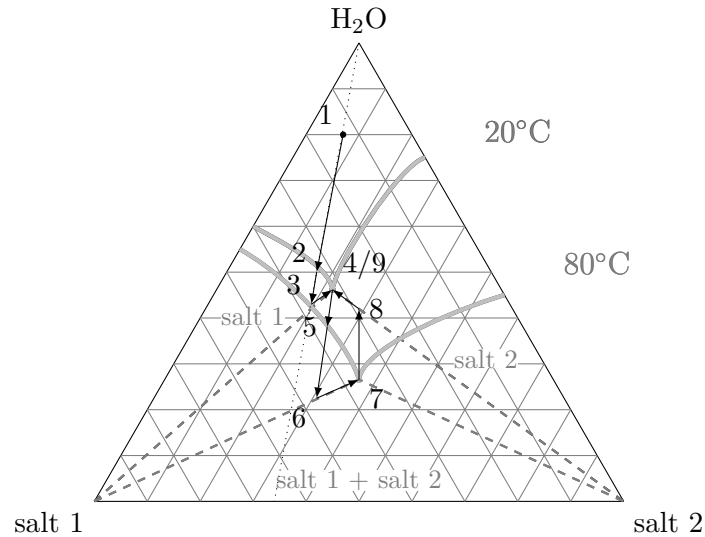
Fig. 15: Basic principle of fractional crystallization in a three component system consisting of two salts in water; Initially, the solution of known composition is relatively dilute, with about 80 % H_2O, 13 % salt 1 and 7 % salt 2 and the temperature is at 20°C (the upper thick gray liquidus line applies) (1); When evaporating water, the composition moves down along a line going from the tip of the triangular plot through the initial composition (dotted line). Initial crystalization of salt 1 starts when the composition crosses the liquidus line (2); Once the composition crosses the tie line (dashed line), additionally salt 2 starts to precipitate (3); Evaporation is stopped and the solid salt 1 is removed from the solution. This causes the total composition to equal the current solution composition, which is the invariant point (4); Now, the system is heated to 80°C, where solubility of both components is elevated (the lower thick gray liquidus line applies). With further evaporation of H_2O, as soon as the liquidus line is crossed, more salt 1 precipitates (5); (6) and (7) are equivalent to (3) and (4); After solid salt 1 was removed, the system is diluted by adding H_2O until the tie line of salt 2 is reached (8); Temperature is lowered back to 20°C and salt 2 precipitates; After removal of solid salt 2, the total composition is again at the invariant point (9); This cycle can be continued as long as sufficient amounts of salts 1 and 2 are present.

A.5. Experimental data for model parametrization

Tab. 7 on page 35 summarizes the availability of experimental data for subsystems of the urine model system. The data was assessed prior to this work and might be of interest for future work. A large data base for electrolyte solutions is the IVC-SEP databank (IVC).

Tab. 7: Summary of availability of solubility data for subsystems relevant to the urine system investigated in this work; o, data available in literature; (o), data availiable, but in limited number or quality; na, no data available in the literature; #, data of special interest for the system investigated in this work

T in °C	Na-NH$_4$-HPO$_4$	Na-NH$_4$-NO$_3$	Na-NH$_4$-SO$_4$	NH$_4$-Cl-HPO$_4$	NH$_4$-SO$_4$-HPO$_4$	(NH$_4$)$_2$HPO$_4$
-20	na	o	o	na	na	na
-10	na	o	o	na	na	na
0	na	o	o	na	o	(o)
10	na	o	o	na	o	(o)
20	na	o	o	na	na	(o)
25	o	o	o	#	o / #	(o)
30	na	o	o	na	na	(o)
40	o	o	o	#	#	(o)
50	na	o	o	na	na	(o)
60	#	o	o	#	#	(o)
70	na	na	o	na	na	(o)
80	#	(o)	(o)	#	#	#
100	#	(o) / #	(o) / #	#	#	#
110	na	(o)	(o)	na	na	na

A.6. Manual for solubility experiments

A method for assessing the solubility of multicomponent electrolyte systems has been developed during a diploma thesis project on a synthetic nitrified urine. This manual gives a detailed description of the method for future reference. Please also refer to the methods and discussion sections of the thesis report for further information regarding analysis and interpretation of the experimental results.

A.6.1. Chemicals

All chemicals used were of grades "purissimum" or "pro analysis", i.e. purities were equal to or greater than 99.0%, from Merk, Sigma-Aldrich and Fluka. Ammonium nitrate had to be purchased from Sigma-Aldrich ($NH_4NO_3 \geq 99\%$, A9642), since the products of other manufacturers contained up to 5% water.

A.6.2. Experimental method

Prior to the experiments, the recipe for the electrolyte solution was determined using the relative composition of salts, in this case from analysis of the composition of urine. An initial water content, at which crystallization was expected to start at room temperature, was determined by simulation using the software EQ3/6 with Pitzer equations (Wolery and Russell, 2003). For the nitrified urine, this was at a concentration factor of 35.7. The recipe for this initial solution was then calculated using the simulated value for alkalinity. Further solutions with lower water content were synthesized by just concentrating the initial solution, e.g. two fold translating to 50% of the water evaporated. Selected recipes are given in **Tab. 8**.

As equilibration vessels, $100\,ml$ bottles (GL45, Schott, Mainz, Germany) with silicon septa (GL45, VWR, Germany) and respective screw cap with aperture (GL45, VWR,

Tab. 8: Recipes for the initial synthetic urine solution (0% evaporated water) and two other concentrations as they were used for the preparation of experiments.

	unit	0%	70%	92.5%
stock solution	g	68.39	33.02	8.78
HCl in stock solution	g	0.806	1.298	1.380
Na_2SO_4	g	5.595	9.006	9.576
$Na_2HPO_4 \cdot 2\,H_2O$	g	7.503	12.077	12.842
NaCl	g	6.341	10.207	10.854
KCl	g	10.509	16.916	17.988
NH_4NO_3	g	47.401	76.298	81.134
mass of water	g	69.1	34.1	10.0
mass of salts	g	76.6	123.3	131.1
total mass of solution	g	145.7	157.5	141.1
water content	%	47.4	21.7	7.1
estimated volume	ml	110	100	80

Germany) were used (**Fig. 16(a)**). The total mass of solution, that was added to the equilibration vessel, was determined by estimating the volume of the solution simply using the densities of water and salts. For the equilibration vessels used, this volume was 100 ml. At the highest concentrations, however, the volume was limited to the apparent density of the salts and had to be lowered down to 80 ml. The total mass of solution was always between 120 and 140 g.

The electrolyte solution was synthesized using salts and a stock solution containing ultra pure water and 32% HCl solution (**Tab. 9**). Salts were weighed to an accuracy of ± 1 mg, the stock solution to ± 50 mg. Salts were added directly to the equilibration vessel one after the other, using plastic weighing dishes. In the end stock solution was added. After adding a magnetic stir bar, the vessel was closed tightly.

The equilibration was done in crystallization beakers of volumes of 1.5 l, which were filled with polypropylen glycole and placed on magnet stirrers, which were connected to contact thermometers (RCT standard, IKA, Staufen, Germany and MR Hei-Tec with EKT 3001, Heidolph, Schwabach, Germany) (**Fig. 16(b)**). One stir bar was put in the oil bath for optimal heat transfer. The temperature accuracy in the oil bath was ± 1°C. Two of these systems were used, each with a maximum capacity of six bottles. The setups were kept under the hood. Ten sets of schott bottles with respective lids were used.

During equilibration, constant mixing was ensured. A speed of around 250 rpm was

(a) Equilibration vessels with different salt concentrations in oil bath; here: 75, 85 and 90% at 80°C (from left to right); The indicated concentrations refer to % H_2O evaporated with respect to the initially simulated concentration.
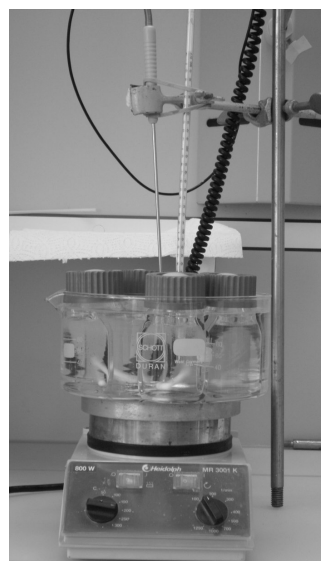
(b) Oil bath on magnet stirrer with temperature probe and equilibration vessels

Fig. 16: Setup of solubility experiments

Tab. 9: Recipes for stock solutions for three different concentrations as used in the prepartion of synthetic urine solutions

	unit	0%	70%	92.5%
HCl 32 %	ml	31.43	104.77	419.08
	g	36.46	121.53	486.13
H_2O	g	953.23	844.1	376.38

found to be optimal. The equilibration times ranged from 60 to 200 h depending on concentrations. Approximately 15 to 30 min before sampling the mother solution, mixing was turned off to allow solids to settle.

A.6.3. Sampling of the mother solution

The mother solution was sampled using 50 ml syringes with long needles (length 200 mm, inner diameter 2 mm, luer lock, Neolab, Heidelberg, Germany) penetrating the septum (**Fig. 17(a)**). An adapter as depicted in **Fig. 17(b)** was put on the back end of the syringe allowing for attaching a vacuum pump (KNFLab Laboport, Trenton, NJ). An additional small needle penetrating the septum was used to balance pressure in the bottle.

In order to prevent solution from accidentally entering the connecting tube to the vacuum pump, cotton wool was put in the opening from the lower end of the vacuum adapter and fixed with tape on the sides. No relevant decrease in sucking performance was observed due to the cotton and the vacuum pump was effectively protected from solution contamination.
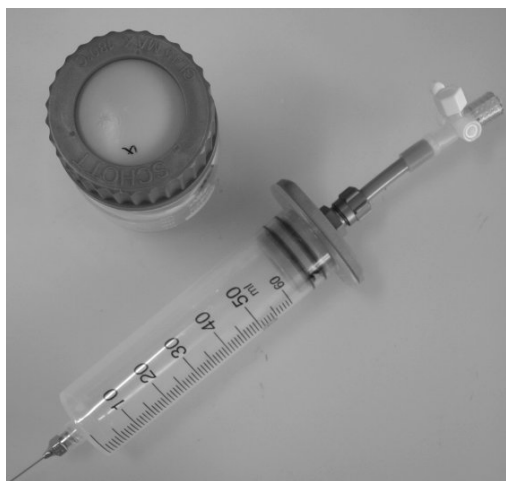
(a) Cap of equilibration vessel with septum and syringe with needle and vacuum adapter

(b) Vacuum adapter with valve manufactured by Eawag workshop

Fig. 17: Equilibration vessels and syringe for sampling mother solution

Before starting to sample, the syringe with attached vacuum adapter and lock at the syringe tip was weighed. The syringe lock was removed and the needle was screwed to the luer lock tightly. The syringe was then connected to the vacuum pump and the latter was turned on. Beforehand, a small needle was punched through the septum off the center. Next, the syringe needle was pushed through the septum center with the sharp edge facing down at a 45° angle, which prevented clogging of the needle with a cut piece of the septum. The needle was then lowered along the vessel wall until just until above the settled crystals with the needle opening facing the wall. This was done to minimize the amount of crystals removed with mother solution (**Fig. 18(a)**). Not more than 50 ml solution was removed at a time to keep space in the syringe to the vacuum adapter.

In a second sampling step, the needle was lowered in the same manner to the lower edge of the vessel to remove as much solution as possible. Tilting the vessel enhanced solution extraction. Usually, two to three sampling steps were sufficient to extract the mother solution.

At the end of a sampling step, the needle was pulled above the solution level with running vacuum pump to suck solution out of the needle. After a few seconds, the valve at the vacuum adapter was closed. The needle was pulled out of the septum and

(a) Needle in equilibration vessel; If crystals are big (e.g. in case of crystallization, i.e. coming from above, or long equilibration time), a crystal cloud forms around the syringe tip, which decreases the amount of crystals sucked in.

(b) Weighing syringe with sampled mother solution using a sample holder; Here the determination of mass of solution sampled is more accurate than using the mass difference of the beaker for dilution before and after sampling.

(c) Diluting sampled mother solution; Pivoting of the syringe prevented clogging in case of strong crystallization in syringe. Also, dipping the syringe tip in the water enhanced evacuation.

Fig. 18: Steps involved in sampling of the mother solution

removed from the syringe and the syringe was immediately closed using the lock. Then, the vacuum adapter was removed from the vacuum pump.

The syringe including the sampled mother solution was weighed (**Fig. 18(b)**) and immediately diluted in 1000 to 1500 g of water (**Fig.18(c)**). In order to allow the solution to discharge, the lock was removed from the syringe and the valve was opened. The syringe evacuated in less than ten seconds. Especially when strong crystallization occured in the syringe at high temperatures, gentle pivoting of the syringe during evacuation prevented clogging of the syringe tip by crystals.

After finishing sampling of the mother solution, the beaker with diluted solution was mixed. Samples for analysis were taken and pH, electric conductivity and density of the solution were determined. For determining the density, a 1 ml pipette was used to sample the solution five times. Each 1 ml sample was weighed and the average was computed.

A.6.4. Sampling of the residue

After complete sampling of the mother solution, the wet residue as a mixture of solids and remaining mother solution in the vessel was kept in the oil bath. In order to sample the residue, vessels were taken from the oil bath and cleaned from oil with hot water from the tab. The vessel was then dried and the cap was removed. The magnetic stir bar was removed and the wet residue was homogenized using a spatula while it was still at high temperature. The vessel with wet residue was weighed to determine the total amount of wet residue. 7 to 20 g of wet residue were transferred to 50 ml tubes for drying.

The wet residue samples were dried by lyophilization in order to prevent any crystal decomposition, which might occur during thermal drying. For this, the tubes containing the wet residues were covered with Parafilm, into which several wholes were punched. They were then either shock frozen in liquid N_2 for around 1 min or put in a freezer at -80°C for at least two hours before putting in the lyophilization apparatus. The samples were dried in average 20 h and the mass loss was determined. Refreezing and lyophilizing was continued until less than 0.1% mass loss was observed. In this way, between 5 and 12 drying steps were required.

A.6.5. Analysis

Samples of mother solution were diluted five to six times and analyzed using ion chromatography (IC). Always two samples of the solution were prepared and analysed. In order to compute the masses of all ions in the mother solution, the initial mass of water in the beaker, in which the mother solution was diluted, the knowledge of the density of the diluted solution and the additional dilution prior to analysis were required. The dried residue was homogenized using a mortar and approximately 1 g was dissolved in 100 ml ultra pure water and analyzed with IC in the same manner than the mother solution.

A.6.6. Problems and recommendations

After turning off stirring before sampling the mother solution, the temperature usually increased by 1-2°C, in few cases up to 4°C. This might be due to stopping the mixing not only in the vessels but also in the oil bath, which lead to non homogeneous temperature distribution.

A deviation for the measurements of K^+ in the residue was found consistently in the analysis, which is described in appendix A.2. These findings must be accounted for in future applications of the method. Using ICP instead of IC for K^+ or all cations might be an adequate solution

Only after having analyzed most of the experiments, it was found that probably a relatively large part of crystals might have been removed when sampling mother solution. The extend of this accidental removal cannot be determined by means of the analysis of the mass balances. The analysis of the results suggests, that in some cases, more than 20 % of solids might have been extracted with solution. The contamination of the residue with solution, however, was still above 70 % by dry mass. Therefore, it is suggested that the focus of extraction of mother solution should lie on not removing solids rather than removing as much solution as possible. This could be achieved by allowing for even longer settling prior to sampling and lowering the needle tip not below the level, where the settled crystals are present.

Using the method described herein, solubility experiments are only possible up to some concentration. For the system investigated here, a water content of 7.1 % at 60°C was really the limit, at which optimal mixing could not be maintained. For such high concentrations, it is not feasible to increase temperature to a level, at which all ions are in equilibrium. Solubility experiments at higher concentrations could be done by distillation. The required experimental work, however, is larger for this method.

Drying the residue samples using freeze drying took often a long time, up to two weeks. This is due to the limited absolute amount of water, that was removed per drying step, even if the sample was kept in the lyophilisator for three days. Lyophilization was initially chosen in order to be sure to not alter the crystal structures of the samples. Since no analysis of the solids such as XRD was applied, thermal drying might have been an alternative, simpler method for drying. However, NH_4NO_3 might decompose at elevated temperatures, which could lead to wrong results.

References

IVC-SEP Databank for Electrolyte Solutions. published online. URL `http://www.cere.dtu.dk/Expertise/Data_Bank.aspx`.

Bernstein, L. Effects of salinity and sodicity on plant growth. *Annual Review of Phytopathology*, 13(1):295–312, 1975. doi:10.1146/annurev.py.13.090175.001455.

Bousmina, F.; Zayani, L.; Ben Hassen-Chehimi, D.; Kbir-Ariguib, N. and Trabelsi-Ayedi, M. Experimental Determination of the Isotherm at 15°C of the System $Mg2^+$, Cl^-, $SO4^-$, H2O. *Monatshefte für Chemie / Chemical Monthly*, 134(5):763–768, April 2003. doi:10.1007/s00706-002-0589-1.

Brouwer, C.; Goffeau, A. and Heibloem, M. *Irrigation Water Management: Training Manual No. 1 - Introduction to Irrigation.* 1985. URL `http://www.fao.org/docrep/R4082E/R4082E00.htm`. Chapter 7, Salty soils.

Cohen-Adad, R. and Cohen-Adad, M.-T. *The Experimental Determination of Solubilities.* John Wiley & Sons, Ltd, 2004. doi:10.1002/0470867833.ch8.

Cohen-Adad, R.; Balarew, C.; Tepavitcharova, S. and Rabadjieva, D. Sea-water solubility phase diagram. Application to an extractive process. *Pure and Applied Chemistry*, 74(10):1811–1821, 2002. ISSN 0033-4545. doi:10.1351/pac200274101811.

Debye, P. and Hückel, E. Zur Theorie der Elektrolyte. I. Gefrierpunktserniedrigung und verwandte Erscheinungen. The theory of electrolytes. I. Lowering of freezing point and related phenomena. *Physikalische Zeitschrift*, 24:185–206, 1923. URL `http://yces.cwru.edu/estir/hist/hist-12-Debye-1.pdf`.

Etter, B.; Tilley, E.; Khadka, R. and Udert, K. M. Low-cost struvite production using source-separated urine in Nepal. *Water Research*, 45(2):852–862, Jan. 2011. doi:10.1016/j.watres.2010.10.007.

European Parliament and European Council. Regulation (EC) no 2003/2003 relating fertilisers, Oct. 2003.

Ganrot, Z.; Dave, G.; Nilsson, E. and Li, B. Plant availability of nutrients recovered as solids from human urine tested in climate chamber on triticum aestivum l. *Bioresource Technology*, 98(16):3122–3129, Nov. 2007. ISSN 09608524. doi:10.1016/j.biortech.2007.01.003.

Germer, J.; Addai, S. and Sauerborn, J. Response of grain sorghum to fertilisation with human urine. *Field Crops Research*, 122(3):234–241, June 2011. ISSN 03784290. doi:10.1016/j.fcr.2011.03.017.

Grattan, S. Salinity–mineral nutrient relations in horticultural crops. *Scientia Horticulturae*, 78 (1-4):127–157, Nov. 1998. ISSN 03044238. doi:10.1016/S0304-4238(98)00192-7.

Keenan, A. G.; Notz, K. and Franco, N. B. Synergistic catalysis of ammonium nitrate decomposition. *Journal of the American Chemical Society*, 91(12):3168–3171, June 1969.

Khlissa, F.; Mnif, A. and Rokbani, R. Application of the conductimetry to the study of the transformation of KCl and Na_2SO_4 into K_2SO_4 between 5 and 30°C. *Chemical Engineering and Processing*, 43(7):929–934, July 2004. doi:10.1016/j.cep.2003.08.002.

Kirchmann, H. and Pettersson, S. Human urine - chemical composition and fertilizer use efficiency. *Nutrient Cycling in Agroecosystems*, 40(2):149–154, Jan. 1995. ISSN 0167-1731. doi:10.1007/BF00750100.

Lide, D. R., editor. *CRC Handbook of Chemistry and Physics, 89th Edition (Internet Version 2009)*. CRC Press/Taylor and Francis, Boca Raton, FL.

Lin, Y.; Kate, A.; Mooijer, M.; Delgado, J.; Fosbøl, P. L. and Thomsen, K. Comparison of activity coefficient models for electrolyte systems. *AIChE J.*, 56(5):1334–1351, 2010. doi:10.1002/aic.12040.

MacNeil, J. H.; Zhang, H.-T.; Berseth, P. and Trogler, W. C. Catalytic decomposition of ammonium nitrate in superheated aqueous solutions. *Journal of the American Chemical Society*, 119(41):9738–9744, Oct. 1997. doi:10.1021/ja971618k.

Maurer, M.; Schwegler, P. and Larsen, T. A. Nutrients in urine: Energetic aspects of removal and recovery. *Water Science and Technology*, 48(1):37–46, 2003.

Maurer, M.; Pronk, W. and Larsen, T. A. Treatment processes for source-separated urine. *Water Research*, 40(17):3151–3166, Oct. 2006. ISSN 00431354. doi:10.1016/j.watres.2006.07.012.

Mir, F. Q. and Shukla, A. Negative rejection of NaCl in ultrafiltration of aqueous solution of NaCl and KCl using sodalite octahydrate zeolite-clay charged ultrafiltration membrane. *Industrial & Engineering Chemistry Research*, 49(14):6539–6546, July 2010. doi:10.1021/ie901775v.

Mnkeni, P. N. S.; Austin, A. and Kutu, F. R. Preliminary studies on the evaluation of human urine as a source of nutrients for vegetables in the eastern cape province, south africa. In *Ecological Sanitation: a Sustainable Integrated Solution. Proceedings of the Third International Ecological Sanitation Conference*, pages 418–426, May 2005.

Mnkeni, P. N. S.; Kutu, F. R.; Muchaonyerwa, P. and Austin, L. M. Evaluation of human urine as a source of nutrients for selected vegetables and maize under tunnel house conditions in the eastern cape, south africa. *Waste Management & Research*, 26(2):132–139, Apr. 2008. doi:10.1177/0734242X07079179.

Munns, R. and Tester, M. Mechanisms of salinity tolerance. *Annual Review of Plant Biology*, 59(1):651–681, 2008. doi:10.1146/annurev.arplant.59.032607.092911.

Oxley, J. Ammonium nitrate: thermal stability and explosivity modifiers. *Thermochimica Acta*, 384(1-2):23–45, Feb. 2002. doi:10.1016/S0040-6031(01)00775-4.

Pitzer, K. S. Thermodynamics of electrolytes. i. theoretical basis and general equations. *The Journal of Physical Chemistry*, 77(2):268–277, Jan. 1973. doi:10.1021/j100621a026.

Platford, P. F. Isopiestic determination of solubilities in mixed salt solutions; two salt systems. *Am J Sci*, 272(10):959–968, December 1972. doi:10.2475/ajs.272.10.959.

Pradhan, S. K.; Pitkanen, S. and Heinonen-Tanski, H. Fertilizer value of urine in pumpkin (cucurbita maxima l.) cultivation. *Agricultural and Food Science*, 19(1):57–67, Mar. 2009. ISSN 1459-6067. doi:10.2137/145960610791015032.

Pronk, W. and Koné, D. Options for urine treatment in developing countries. *Desalination*, 248(1-3):360–368, Nov. 2009. ISSN 00119164. doi:10.1016/j.desal.2008.05.076.

Qadir, M. and Schubert, S. Degradation processes and nutrient constraints in sodic soils. *Land Degrad. Dev.*, 13(4):275–294, 2002. doi:10.1002/ldr.504.

Qadir, M.; Ghafoor, A. and Murtaza, G. Amelioration strategies for saline soils: a review. *Land Degrad. Dev.*, 11(6):501–521, 2000. doi:10.1002/1099-145X(200011/12)11:6%3C501::AID-LDR405%3E3.0.CO;2-S.

R Development Core Team. *R: A Language and Environment for Statistical Computing.* R Foundation for Statistical Computing, Vienna, Austria, 2003. URL `http://www.R-project.org/`. ISBN 3-900051-07-0.

Richards, L. A., editor. *Diagnosis and Improvement of Saline and Alkali Soils. USDA Handbook No. 60. US Government Printing Office: Washington, DC.*, volume 60. U.S. Deptartment of Agriculture, 1954.

Rubtsov, Y. I.; Strizhevskii, A. I. and Kazakov, A. I. Possibilities of lowering the rate of thermal decomposition of AN. *Zhurnal Prikladnoi Khimii*, 62:2169–2174, 1989.

Saunders, H. L. Lxxxi.-the decomposition of ammonium nitrate by heat. *J. Chem. Soc., Trans.*, 121:698–711, 1922. doi:10.1039/CT9222100698.

Scatchard, G.; Hamer, W. J. and Wood, S. E. Isotonic Solutions. I. The Chemical Potential of Water in Aqueous Solutions of Sodium Chloride, Potassium Chloride, Sulfuric Acid, Sucrose, Urea and Glycerol at 25°C. *Journal of the American Chemical Society*, 60(12):3061–3070, December 1938. doi:10.1021/ja01279a066.

Schouw, N. L.; Danteravanich, S.; Mosbaek, H. and Tjell, J. C. Composition of human excreta - a case study from southern thailand. *Science of The Total Environment*, 286(1-3):155–166, Mar. 2002. ISSN 00489697. doi:10.1016/S0048-9697(01)00973-1.

Simons, J. and Clemens, J. The use of separated human urine as mineral fertilizer. In *2nd international symposium on ecological sanitation*, page 595, Apr. 2003.

Soil Science Society of America. Glossary of soil science terms, 1997. URL `https://www.soils.org/publications/soils-glossary`.

Suarez, D. L. UNSATCHEM: Unsaturated water and solute transport model with equilibrium and kinetic chemistry. *Soil Science Society of America Journal*, 61(6):1633–1646, 1997. ISSN 0361-5995.

Thomsen, K. *Aqueous electrolytes: model parameters and process simulation.* PhD thesis, Technical University of Denmark, 1997.

Thomsen, K.; Rasmussen, P. and Gani, R. Correlation and prediction of thermal properties and phase behaviour for a class of aqueous electrolyte systems. *Chemical Engineering Science*, 51 (14):3675–3683, 1996. doi:10.1016/0009-2509(95)00418-1.

Udert, K. M. and Wächter, M. Complete nutrient recovery from source-separated urine by nitrification and distillation. Submitted, 2011.

Udert, K. M.; Fux, C.; Münster, M.; Larsen, T. A.; Siegrist, H. and Gujer, W. Nitrification and autotrophic denitrification of source-separated urine. *Water Science and Technology*, 48(1): 119–130, 2003a. doi:10.1021/es048422m.

Udert, K. M.; Larsen, T. A.; Biebow, M. and Gujer, W. Urea hydrolysis and precipitation dynamics in a urine-collecting system. *Water Research*, 37(11):2571–2582, June 2003b. ISSN 00431354. doi:10.1016/S0043-1354(03)00065-4.

Udert, K. M.; Larsen, T. A. and Gujer, W. Chemical Nitrite Oxidation in Acid Solutions as a Consequence of Microbial Ammonium Oxidation. *Environmental Science & Technology*, 39 (11):4066–4075, June 2005. doi:10.1021/es048422m.

Udert, K. M.; Larsen, T. A. and Gujer, W. Fate of major compounds in source-separated urine. *Water Science and Technology*, 54(11-12):413–420, 2006.

Volkmar, K. M.; Hu, Y. and Steppuhn, H. Physiological responses of plants to salinity: A review. *Canadian Journal of Plant Science*, 78(1):19–27, 1998.

Wolery, T. and Russell, L. *SOFTWARE USER'S MANUAL EQ3/6, Version 8.0*. U.S. Department of Energy, Office of Civilian Radioactive Waste Management, Las Vegas, NA, 2003. ISBN 3-900051-07-0.

Wood, B. F. and Wise, H. Acid catalysis in the thermal decomposition of ammonium nitrate. *The Journal of Chemical Physics*, 34(4):693–696, 1955.

Affirmation

Herewith I affirm that I have written this thesis on my own and that I did not use any other resources and references than those cited.

Hiermit versichere ich, die vorliegende Diplomarbeit selbstständig verfasst und keine weiteren als die angegebenen Hilfsmittel und Quellen benutzt zu haben.

Dübendorf, September 9, 2011